

# CuraView: A Multi-Agent Framework for Medical Hallucination Detection with GraphRAG-Enhanced Knowledge Verification

**Severin Ye\***

*School of Computer Science and Engineering  
Kyungpook National University  
Daegu, Republic of Korea  
6severin9@gmail.com*

**Xiaopeng He<sup>‡</sup>**

*West China School of Medicine  
Sichuan University  
Chengdu, China  
hxp19180945016@stu.wchscu.cn*

**Xiao Kong\***

*School of Computer Science and Engineering  
Kyungpook National University  
Daegu, Republic of Korea  
kongx7546@knu.ac.kr*

**Guangsu Yan<sup>‡</sup>**

*School of Aerospace Science and Engineering  
Shandong University  
Weihai, China  
202300800569@mail.sdu.edu.cn*

**Dongsuk Oh<sup>†</sup>**

*Department of English Language and Literature,  
Kyungpook National University, Daegu, Republic  
of Korea  
inow3555@knu.ac.kr*

\*Co-first authors with equal contribution; †Corresponding author; ‡Co-second authors

## Abstract

Discharge summaries require extracting critical information from lengthy electronic health records (EHRs), a process that is labor-intensive when performed manually. Large language models (LLMs) can improve generation efficiency; however, they are prone to producing faithfulness hallucinations—statements that contradict source records—posing direct risks to patient safety. To address this, we present *CuraView*, a multi-agent framework for sentence-level detection and evidence-grounded explanation of faithfulness hallucinations in discharge summaries. CuraView constructs a GraphRAG-based knowledge graph from patient-level EHRs and implements a closed-loop generation–detection pipeline with sentence-level evidence retrieval and classification spanning four evidence grades from strong support to direct contradiction (E1–E4), yielding structured and interpretable evidence chains.

We evaluate CuraView on a subset of 250 patients from the Discharge-Me benchmark, with 50 patients held out for testing. Our fine-tuned Qwen3-14B detection model achieves an F1 of 0.831 on the safety-critical E4 metric (90.9% recall, 76.5% precision) and an F1 of 0.823 on E3+E4, representing a 50.0% relative improvement over the base model and outperforming RAGTruth-style and QAGS-style baselines. These results demonstrate that evidence-chain-based graph retrieval verification substantially improves the factual reliability of clinical documentation,

while simultaneously producing reusable annotated datasets for downstream model training and distillation.

keywords: discharge summary generation, faithfulness hallucination, hallucination detection, GraphRAG, knowledge graph, electronic health records, patient safety, clinical NLP

## 1 Introduction

Large language models (LLMs) have demonstrated strong potential across medical applications, particularly in clinical documentation tasks such as discharge summary generation, diagnostic assistance, and radiology report generation [1][2]. Landmark models including Med-PaLM and Med-PaLM 2 achieved 67.6% and 86.5% accuracy on USMLE-style questions in the MedQA benchmark, respectively [3][4], while GPT-4 demonstrated competitive performance on the MultiMedQA benchmark [5]. Among clinical documentation tasks, discharge summary generation is of particular safety significance: discharge summaries serve as the primary record guiding post-discharge medication, follow-up care, and inter-provider communication, and errors introduced at this stage propagate directly into downstream clinical decisions [6][7]. Despite this promise, a fundamental barrier to clinical adoption remains: *faithfulness hallucinations*—statements generated by LLMs that contradict source records. Unlike hallucinations in general-domain applications, medical hallucinations pose direct risks to patient safety: a single medication dosage error can be fatal, a missed cancer diagnosis may delay life-saving treatment, and fabricated laboratory results may trigger unnecessary interventions [2][8][9]. If generated content cannot be consistently verified against patient-level evidence, clinicians and institutions are unlikely to rely on LLM outputs in real clinical workflows.

Hallucination rates, error patterns, and risk profiles vary substantially across clinical tasks [10][7][6][11][12], making task-specific detection mechanisms essential. This work focuses on faithfulness hallucinations in discharge summary generation—specifically, statements that contradict information documented in a patient’s electronic health record (EHR). It does not address general medical question-answering correctness or query-level evaluation; rather, it studies patient-grounded sentence-level claim verification for clinical documentation. Through systematic analysis of clinical documentation errors, we identify seven hallucination types spanning diagnosis, medication, laboratory results, temporal information, numerical values, negation, and fabricated facts (Section 2.2).

Current approaches to medical hallucination detection exhibit four limitations that motivate this work. **L1 (Lack of systematic generation):** Existing benchmarks such as Med-HALT [10] rely on costly manual annotation; no prior work provides an automated framework for generating diverse medical errors at scale. **L2 (Missing patient-specific context):** Most research evaluates hallucinations against generic corpora rather than individualized EHR evidence [13][14], making it impossible to verify patient-specific claims such as medication allergies or current prescriptions. **L3 (Insufficient evidence support):** Detection methods rarely provide structured, interpretable explanations grounded in specific EHR records [7][6], limiting the development of auditable detection pipelines. **L4 (Evaluation-only focus):** Prior work measures hallucination rates but does

not provide end-to-end systems for generation, detection, and explanation in operational settings [10].

To address these limitations, we present **CuraView**, a multi-agent framework for medical hallucination detection with GraphRAG-enhanced knowledge verification. The primary objective of CuraView is sentence-level detection and evidence-grounded explanation of faithfulness hallucinations in discharge summaries; the generation agent constructs controlled training and evaluation samples rather than defining the final clinical deployment target. We use GraphRAG [15] rather than standard retrieval-augmented generation (RAG) [16] because clinical verification requires recovering relational structure across diagnoses, medications, laboratory results, and temporal records—relationships that flat document retrieval cannot reliably capture. GraphRAG organizes distributed multi-table EHR evidence into a queryable relational graph, enabling sentence-level factual verification with explicit evidence chains. CuraView addresses each limitation directly: an automated hallucination generation module covering seven error types (L1); patient-specific knowledge graph construction from multi-table EHRs (L2); an interpretable E1–E4 evidence grading scheme (L3); and a complete generation–detection–evaluation pipeline (L4). Figure 1 summarizes this end-to-end pipeline and its three core cooperating components; the methodology section expands each stage in detail.

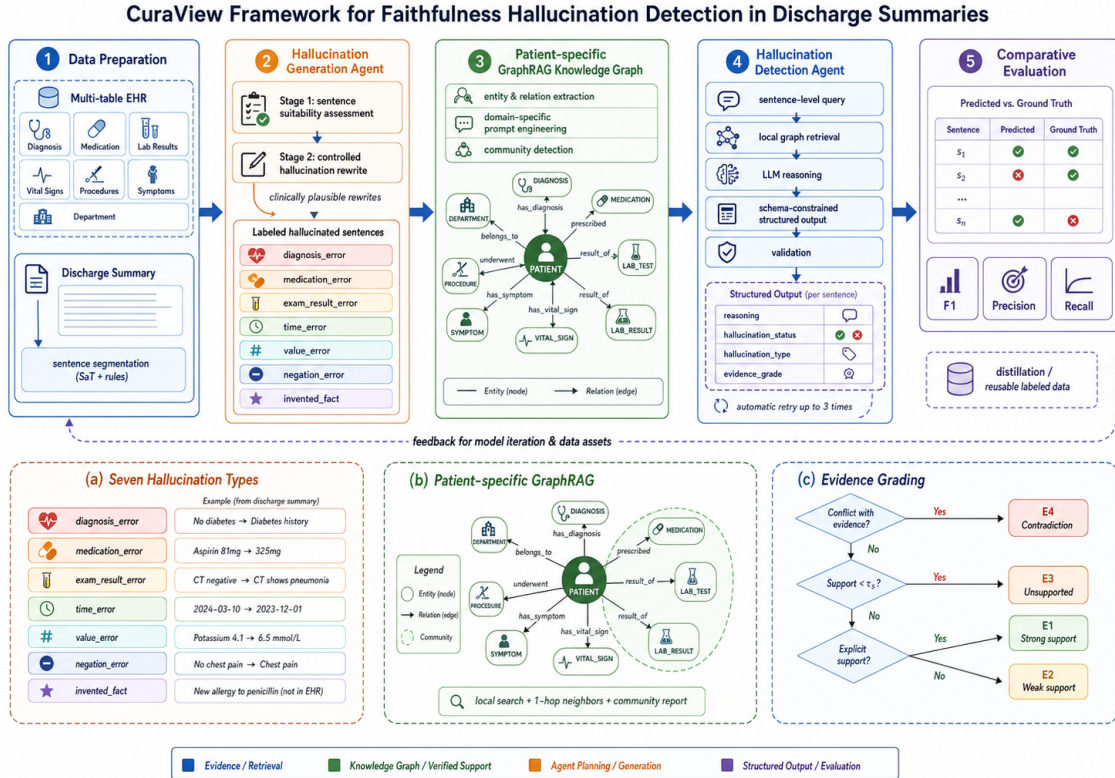


Figure 1: CuraView System Architecture Overview. The framework comprises three core components working in concert: the hallucination generation agent based on LangChain systematically generates medical errors; the GraphRAG knowledge graph constructs patient-specific knowledge bases from EHRs; the hallucination detection agent leverages knowledge graphs for evidence verification.

Our key contributions are as follows:

- **A clinically grounded hallucination taxonomy (addresses L1).** We define **seven** hallucination types covering the full spectrum of documentation errors in discharge summaries—from diagnosis and medication errors to fabricated facts—enabling automated, fine-grained sentence-level annotation across **1,103** test sentences derived from real EHRs.
- **An end-to-end multi-agent framework (addresses L4).** Unlike prior systems such as MedAgents [17] that target diagnosis support using general medical knowledge bases, CuraView employs an adversarial generation–detection architecture focused on hallucination quality control over patient-specific EHR evidence, achieving **F1 = 0.831** on safety-critical E4 hallucinations—a **50.0%** relative improvement over the base model.
- **GraphRAG-based patient-specific knowledge graphs (addresses L2).** Domain-customized prompt engineering reduces per-patient entity count by **75.8%** (from 240 to 58 entities) and achieves full graph connectivity (from 7 disconnected components to 1), yielding

a **43.0%** improvement in downstream detection F1 compared to graphs constructed without domain adaptation.

- **A unified structured output reliability pipeline (addresses L3).** A three-layer schema-constrained validation pipeline—combining Pydantic type checking, JSON repair, and consistency verification [18][19][20][21]—enables **14B** models to achieve near-100% JSON parsing success under strict output constraints, compared to only **40–50%** for 8B models under identical settings, ensuring stable downstream batch processing across both API and local deployments.
- **Comprehensive empirical evaluation.** Evaluated on **50** held-out patients (**1,103** sentences) from the Discharge-Me benchmark [22][23], CuraView outperforms RAGTruth-style (F1 = 0.639) and QAGS-style (F1 = 0.631) baselines by **+0.192** and **+0.200** in F1, respectively, while maintaining 90.9% recall on safety-critical E4 hallucinations.

## 2 Problem Formulation

### 2.1 Definition of Hallucination

In the context of large language models, *hallucination* refers to the phenomenon where model-generated content appears plausible but actually contradicts established knowledge or source documents [9]. Ji et al. categorized hallucinations into two types: *factual hallucinations* (contradicting established knowledge) and *faithfulness hallucinations* (inconsistent with source documents). In the medical context, both types carry serious patient safety implications.

This work focuses on **faithfulness hallucinations** in clinical documentation generation—specifically, statements in discharge summaries that contradict information recorded in a patient’s EHR. This focus is motivated by the directness of the verification path: faithfulness hallucinations can in principle be detected by comparing generated text against structured patient records, making them amenable to evidence-grounded automated detection. The task is therefore not general medical diagnosis evaluation or open-ended query answering, but patient-specific verification of clinical statements against source records. The hallucination taxonomy and evidence grading system introduced below define the precise scope of detection targeted by CuraView.

### 2.2 Medical Hallucination Taxonomy

Based on systematic analysis of error patterns in clinical documentation, we classify medical hallucinations into seven types organized by clinical risk profile.

The three highest-risk types involve direct conflicts with documented clinical facts. **Diagnostic errors** involve misidentification of disease (e.g., “pneumonia” rewritten as “tuberculosis”), which may lead to entirely incorrect treatment plans. **Medication errors** cover incorrect drug names or dosages (e.g., “aspirin 81 mg” rewritten as “aspirin 325 mg”), where dosage discrepancies can cause drug toxicity or treatment failure. **Test result errors** involve fabricated or incorrect laboratory

values (e.g., “blood glucose 96 mg/dL” rewritten as “196 mg/dL”), which may trigger unnecessary emergency interventions or mask genuine abnormalities.

Two further types introduce errors that are clinically significant but may be less immediately apparent. **Numerical errors** affect vital sign values (e.g., “blood pressure 120/80 mmHg” rewritten as “180/120 mmHg”), potentially triggering erroneous emergency responses. **Negation errors** reverse affirmative or negative relationships (e.g., “no history of diabetes” rewritten as “history of diabetes”), which can fundamentally alter risk assessment despite appearing as a minor textual change.

The remaining two types address temporal and fabrication patterns. **Temporal errors** introduce inconsistencies in time references (e.g., “admitted yesterday” rewritten as “admitted last week”), affecting understanding of disease progression and treatment timing. **Fabricated facts** are entirely invented clinical events with no basis in the patient’s records (e.g., adding a non-existent appendectomy); unlike the preceding types, these errors cannot be verified by direct contradiction but should be flagged as suspicious based on the absence of supporting evidence. Representative examples for all seven types are provided in Table 4.

This taxonomy differs from prior work [9, 10] in two respects: it focuses specifically on **sentence-level faithfulness errors** in clinical documentation rather than question-answering accuracy, and it grounds each error type in **patient-specific EHR evidence** rather than population-level medical knowledge.

For clarity, we formalize the taxonomy as follows. For a patient  $p$ , let  $E_p$  denote the set of structured and unstructured EHR evidence available for verification. A discharge summary is segmented into sentences  $\{s_i\}_{i=1}^n$ , and each sentence may contain one or more clinical claims. GraphRAG retrieves an evidence context  $C_i \subseteq E_p$  for sentence  $s_i$ . The type space is  $T = \{\text{diagnosis\_error, medication\_error, exam\_result\_error, time\_error, value\_error, negation\_error, invented\_fact}\}$ . To allow multiple clinical errors within the same sentence, sentence-level type identification is represented as a type set:

$$H(s_i, C_i) = \{t \in T \mid \phi_t(s_i, C_i) = 1\},$$

where  $\phi_t(s_i, C_i)$  is the decision predicate associated with type  $t$ . If  $H(s_i, C_i) = \emptyset$ , none of the seven hallucination types is detected; otherwise, each element in  $H(s_i, C_i)$  corresponds to an identified error type. The seven predicates are defined as follows:

- $\phi_{\text{diagnosis}}(s_i, C_i) = 1$ : the diagnosis entity or disease status in the sentence conflicts with the patient’s diagnosis records, clinical course, or related EHR evidence.
- $\phi_{\text{medication}}(s_i, C_i) = 1$ : the medication name, dosage, frequency, or medication status conflicts with the patient’s medication record.
- $\phi_{\text{exam}}(s_i, C_i) = 1$ : the laboratory test, radiology finding, or examination result conflicts with the corresponding EHR evidence.
- $\phi_{\text{time}}(s_i, C_i) = 1$ : the temporal expression, event ordering, or duration conflicts with the

timeline documented in the patient record.

- $\phi_{\text{value}}(s_i, C_i) = 1$ : a vital sign, numerical measurement, or quantitative description conflicts with a recorded EHR value.
- $\phi_{\text{negation}}(s_i, C_i) = 1$ : an affirmative or negative relationship is reversed relative to the patient record.
- $\phi_{\text{invented}}(s_i, C_i) = 1$ : the sentence contains a clinically relevant claim for which no supporting patient evidence can be retrieved and no direct conflicting evidence is available.

The first six predicates correspond primarily to direct conflicts between a claim and patient evidence, whereas  $\phi_{\text{invented}}$  captures clinically relevant claims without patient-level support. This type set is paired with the evidence grading function  $g(s_i, C_i) \rightarrow \{E1, E2, E3, E4\}$  defined below.

### 2.3 Evidence Grading System

To quantify both the detectability and the clinical impact of hallucinations, we introduce a four-level evidence grading system. **E1 (Strong Support)** denotes statements with explicit EHR evidence, such as matching diagnostic codes, medication records, or laboratory results in the patient’s structured records. **E2 (Weak Support)** denotes statements supported only indirectly—for example, a claim that “the patient has diabetes” may be graded E2 when the patient is on long-term metformin therapy, even if no explicit diabetes diagnosis code is present. **E3 (No Support)** denotes statements absent from the EHR evidence that should nonetheless be flagged as problematic based on contextual judgment; typical cases include entirely fabricated events or facts not present anywhere in the medical record. **E4 (Contradiction)** denotes statements that directly contradict explicit factual evidence in the EHR, such as diagnoses, medications, laboratory values, or negation relationships inconsistent with the records; this is the most critical safety level, representing errors definitively identifiable from evidence.

Formally, let  $\text{conflict}(s_i, C_i)$  indicate whether the sentence directly contradicts the evidence context,  $\text{support}(s_i, C_i)$  denote evidence support strength,  $\tau_s$  denote the support threshold, and  $\text{explicit}(s_i, C_i)$  indicate whether support comes from explicit structured or textual records. The evidence grading function is defined as:

$$g(s_i, C_i) = \begin{cases} E4, & \text{conflict}(s_i, C_i) = 1, \\ E3, & \text{conflict}(s_i, C_i) = 0 \wedge \text{support}(s_i, C_i) < \tau_s, \\ E2, & \text{support}(s_i, C_i) \geq \tau_s \wedge \text{explicit}(s_i, C_i) = 0, \\ E1, & \text{support}(s_i, C_i) \geq \tau_s \wedge \text{explicit}(s_i, C_i) = 1. \end{cases}$$

This work focuses on detecting **E3** and **E4** hallucinations, as these two grades represent clinical statements that require systematic verification before a discharge summary can be considered trustworthy. Among these, E4 is treated as the primary safety-critical outcome—errors at this level are directly contradicted by patient records and pose the most immediate risk—while E3 serves as a supplementary broad-coverage metric capturing suspicious statements that lack evidential support.

## 3 Related Work

Before detailing the CuraView methodology, we survey existing research on medical hallucination detection, knowledge graph-augmented generation, and multi-agent systems to establish the positioning and novelty of this work.

### 3.1 Hallucination in Medical Large Language Models

#### 3.1.1 Capabilities and Limitations of Medical Large Language Models

While recent medical LLMs including Med-PaLM [3], Med-PaLM 2 [4], GPT-4 [5], Clinical Camel [24], and PMC-LLaMA [25] have achieved strong benchmark performance on medical question-answering tasks, benchmark accuracy does not translate directly to clinical reliability. Ji et al. [9] provided a comprehensive survey of hallucinations in natural language processing, categorizing them into *factual hallucinations* (contradicting established knowledge) and *faithfulness hallucinations* (inconsistent with source documents). In the medical context, both types pose serious risks; however, none of the above models provide mechanisms for verifying generated content against patient-level EHR evidence, leaving generated content unverifiable against patient-level evidence in deployment.

#### 3.1.2 Medical Hallucination Benchmarks

**Med-HALT** [10] introduced the first systematic medical hallucination benchmark, covering 1,755 questions across five medical specialties. Even state-of-the-art models such as GPT-4 exhibited hallucination rates of 10–15% on factual medical questions, and hallucinations frequently accompanied high confidence scores, making them particularly dangerous in clinical settings. However, Med-HALT focuses exclusively on question-answering scenarios and provides no mechanism for patient-specific verification or structured error explanation—limitations that directly motivate L1 and L3 of this work. **Asgari et al.** [7] advanced evaluation granularity from question-level accuracy to sentence-level clinical summary safety assessment. Among 12,999 clinician-annotated sentences, they reported sentence-level hallucination rates of 1.47% and omission rates of 3.45%, with 44% of hallucinations classified as critical errors. While this work establishes that even low absolute error rates carry significant clinical risk, it does not provide patient-grounded explanations for detected errors, leaving the causal evidence opaque to clinicians. **Williams et al.** [6] examined discharge summary narrative generation, comparing inaccuracy, omission, and hallucination as three error categories. LLM-generated versions contained an average of 2.91 unique errors per document, compared to 1.82 in physician-authored versions, suggesting that “errors per document” is a more appropriate risk metric than a single sentence-level hallucination rate in this setting. Neither Asgari et al. nor Williams et al. provide structured, patient-grounded explanations that clarify *why* a statement is incorrect or *what EHR evidence* contradicts it—a gap that CuraView’s evidence grading scheme directly addresses by linking each detected error to specific EHR records (Section 2.2). The **Discharge Me** shared task advanced discharge summary generation to a unified

benchmark [22]. Among submissions, EPFL-MAKE used MEDISCHARGE based on Meditron-7B with context window expansion and dynamic information selection [26]; UF-HOBI adopted a two-stage hybrid pipeline combining clinical concept extraction with coherent paragraph generation [27]. These works demonstrate a relatively mature generation pipeline, but none addresses patient-level fact verification or hallucination explanation, confirming the gap identified in L4.

In **radiology report generation**, hallucination risks are more pronounced. **Artsi et al.** [11] conducted a systematic review of 15 studies and found that all models exhibited varying degrees of hallucinations, misdiagnoses, or report inconsistencies, with missing clinical details reported in 12 of 15 studies. **RadFlag** [12] provided sentence-level hallucination detection for radiology reports, finding that approximately 40% of generated sentences in high-performing models may contain hallucinations, with high-risk reports averaging 4.2 true hallucinations versus 1.9 in accepted reports. While RadFlag demonstrates the value of black-box sentence-level detection, it is designed specifically for radiology report generation and does not extend to multi-table EHR evidence verification for discharge summaries.

In summary, existing literature supports a task-dependent, evaluation-granularity-dependent understanding of medical hallucination: error rates, risk profiles, and evaluation metrics are not directly comparable across question-answering, clinical summaries, discharge summaries, and radiology reports. The taxonomy proposed in Section 2.2 focuses on sentence-level faithfulness errors in clinical documentation, emphasizing alignment with patient-specific EHR evidence and thus complementing prior work on question-answering and radiology.

Table 2 summarizes how these datasets and tasks differ from the setting addressed in this work.

<b>Dataset / Work</b>	<b>Original task</b>	<b>Hallucination focus</b>	<b>Granularity</b>	<b>Patient-level EHR grounding</b>
Med-HALT [10]	Medical question answering	Factual medical QA hallucination	Question level	No
Asgari et al. [7]	Clinical summary safety evaluation	Hallucination and omission in summaries	Sentence level	Clinical-summary evidence
Williams et al. [6]	Discharge narrative quality assessment	Inaccuracy, omission, hallucination	Document / error level	Discharge-summary review
RadFlag [12]	Radiology report hallucination detection	Radiology-specific hallucination	Sentence level	Radiology-report context
Discharge-Me [22]	Clinical text generation shared task	Not originally a hallucination benchmark	Section / document generation	Provides MIMIC-IV-derived patient records

<b>Dataset / Work</b>	<b>Original task</b>	<b>Hallucination focus</b>	<b>Granularity</b>	<b>Patient-level EHR grounding</b>
CuraView	Patient-grounded discharge- summary verification	Faithfulness hallucination against EHR evidence	Sentence level with E1–E4 evidence grades	Yes

*Positioning of CuraView relative to representative medical hallucination and clinical text generation datasets.*

## 3.2 Knowledge Graphs and Retrieval-Augmented Generation

### 3.2.1 Foundations of Retrieval-Augmented Generation

Retrieval-augmented generation (RAG) [16] introduced a paradigm shift in LLM applications by combining neural retrieval with language generation, significantly improving performance on knowledge-intensive tasks such as open-domain question-answering. Subsequent work extended RAG to fact verification and domain-specific question-answering: **RARR** [28] combined retrieval with refinement to correct LLM outputs using external evidence; **MedRAG** [29] benchmarked medical RAG configurations through the MIRAGE benchmark; **BioRAG** [30] combined large-scale scientific literature with domain-specific embeddings to support biomedical question reasoning.

Although these works demonstrate clear value of retrieval augmentation in professional domains, they are built on *flattened document retrieval*, which is insufficient for explicitly modeling structured relationships among medical concepts. In discharge summary verification, for instance, the system must do more than retrieve a sentence stating that a patient is taking a medication; it must also relate that medication to allergy history, discontinuation records, or abnormal laboratory findings documented in separate EHR tables—cross-source relationships that flat retrieval routinely fails to recover. This limitation motivates the shift to graph-structured retrieval as the foundation for patient-specific evidence verification.

### 3.2.2 GraphRAG: Graph-Structured Retrieval Augmentation

Microsoft’s **GraphRAG** [15] addresses the limitation of traditional RAG in modeling document structural relationships by converting documents into knowledge graphs before retrieval. The method employs a two-level indexing architecture: entity-level indices for local search over specific entities and their direct relationships, and community-level indices for global search, aggregating knowledge from clusters detected by the Leiden algorithm. Compared to standard RAG, this graph-structured approach captures complex multi-hop reasoning relationships and discovers thematic patterns through community structure.

In medical contexts, **Medical Graph RAG** [31] further demonstrates that connecting patient documents to trustworthy medical sources via graph retrieval can significantly enhance evidence reliability. Medical RAG system surveys confirm that external knowledge sources are an important path for mitigating hallucinations and enhancing transparency [32]. Together, these results explain why GraphRAG is more suitable than retrieval-free or flat-retrieval approaches as the methodological foundation for patient-specific evidence verification.

### 3.2.3 Medical Knowledge Graphs

Standard medical ontologies—including UMLS [33], which integrates over 200 medical terminology sets for semantic interoperability; SNOMED-CT [34], a comprehensive clinical terminology system with hierarchical relationships; and ICD-10 [35], the international disease classification standard—provide structured representations of population-level clinical knowledge, but lack the patient-specific information necessary for individualized verification.

Prior work on EHR-based knowledge graph construction has demonstrated the feasibility of extracting structured knowledge from clinical records: Rotmensch et al. [13] automatically constructed disease knowledge graphs from EHR data via ICD codes and clinical notes, while Finlayson et al. [14] developed entity linking methods to align clinical note mentions with UMLS concepts. Recent surveys on integrating SNOMED CT with LLMs further show that terminological knowledge injected through input augmentation or retrieval-based fusion improves downstream NLP performance [36]. However, these approaches aggregate knowledge across patients rather than organizing evidence around a single patient’s actual records, making them unsuitable for the individualized verification task addressed in this work.

Key challenges in medical knowledge graph construction include handling terminology variants such as abbreviations and colloquialisms in clinical notes, modeling the temporal evolution of disease progression and treatment history, and balancing cross-patient knowledge aggregation with privacy protection. CuraView addresses these challenges through domain-customized prompt engineering and patient-level graph isolation, as detailed in Section 4.

### 3.2.4 Positioning of Our Approach

CuraView differs from prior work on four dimensions.

**Patient-Specific Knowledge Graphs.** Existing medical knowledge graphs—whether ontological resources such as UMLS [33] or EHR-derived graphs such as those in Rotmensch et al. [13]—are population-level constructs that aggregate knowledge across patients. Medical Graph RAG [31] connects patient documents to general medical sources but does not construct individualized per-patient graphs from multi-table EHR data. CuraView instead builds a separate knowledge graph for each patient, grounding all verification in that patient’s actual records and eliminating cross-patient contamination.

**Verification-Oriented Evidence Semantics.** Prior hallucination detection work reports binary hallucination labels or aggregate error rates [7, 10], but does not provide structured evidence

grading that explains the *degree* of support or contradiction between a claim and its source records. CuraView addresses this gap through a four-level evidence grading scheme that links each detection decision to specific EHR records, producing clinician-readable audit trails (Section 2.2).

**Multi-Table EHR Integration.** Existing approaches typically operate on a single data source—clinical notes [14] or ICD codes [13]—and cannot perform cross-source relationship reasoning. CuraView unifies heterogeneous EHR sources including diagnoses, medications, laboratory results, vital signs, radiology reports, and triage records into a single patient knowledge graph, enabling verification across all available evidence simultaneously.

**Dynamic Patient-Grounded Evidence Organization.** Static general-purpose ontologies cannot reflect the temporal evolution of an individual patient’s condition. CuraView organizes evidence dynamically around each patient’s actual records, supporting temporal relationship modeling and enabling detection of time-sensitive errors such as medication discontinuation inconsistencies—error types that static ontologies cannot address.

### 3.3 Multi-Agent Systems and LLM Applications

#### 3.3.1 LLM Agent Frameworks

**LangChain** [18] provides a modular framework including prompt templates, LLM wrappers, tool-calling interfaces, and memory management; CuraView’s generation and detection agents are built on LangChain 1.0 to ensure scalability. **AutoGPT** [37] demonstrated autonomous goal decomposition with long-term memory and internet access. **ReAct** [38] introduced the “reasoning + action” paradigm, alternating between chain-of-thought and tool-calling in iterative reasoning.

Recent agent research shows that on structured subtasks such as function calling and workflow orchestration, smaller models optimized through task-specific training can match or exceed larger general-purpose models [39][40][41]. This finding informed our choice of Qwen3-14B as the primary local detection model, prioritizing task-specific fine-tuning and structured output stability over raw parameter scale (Section 5).

#### 3.3.2 Comparison with Existing Work

Among existing medical multi-agent systems, **MedAgents** [17] represents the state of the art for zero-shot medical reasoning, employing multiple LLM agents that collaborate using general medical knowledge bases such as PubMed and clinical textbooks. However, MedAgents and similar systems face two critical limitations in patient-specific scenarios: they cannot leverage individualized EHRs for precise reasoning, and they lack systematic detection mechanisms for hallucination in generated content.

Methodologically, CuraView’s dual-agent design combines two emerging directions. First, adversarial sample generation continually constructs challenging errors, improving detector robustness against diverse error types. Second, the LLM-as-a-judge paradigm [42][43] suggests that evidence-centered structured evaluation is better suited to high-risk quality control than a single open-ended

response. The separation between CuraView’s generation agent and detection agent is therefore not merely an engineering decomposition, but a principled design supporting two complementary objectives: producing hard cases and performing evidence-driven verification.

CuraView achieves key distinctions on four dimensions compared to prior medical agent systems. **(1) Task Positioning:** CuraView is, to our knowledge, the first multi-agent system focused specifically on hallucination detection and quality control in clinical documentation, rather than diagnosis or treatment support. **(2) Knowledge Sources:** Rather than relying on generalized medical literature, CuraView constructs patient-specific EHR knowledge graphs that provide individualized, verifiable evidence. **(3) Agent Collaboration:** The adversarial generation–detection architecture systematically challenges detector robustness with diverse generated error samples, producing a self-improving quality control loop. **(4) Data Contribution:** The adversarial process simultaneously produces annotated training and distillation data, creating reusable resources for future medical LLM safety research.

Compared to existing medical agent systems that operate primarily at the level of prompt engineering or single-model output, CuraView emphasizes the end-to-end usability of structured outputs—specifically, whether generation results can reliably enter downstream verification, evaluation, and batch processing workflows without manual intervention. The concrete mechanisms enabling this, including schema-constrained generation, multi-layer validation, and automatic retry logic, are detailed in Section 4.

## 4 Methodology

### 4.1 System Architecture Overview

CuraView is an end-to-end medical hallucination detection framework comprising three core components that operate in a closed-loop pipeline. The **hallucination generation agent**, built on LangChain 1.0 [18], systematically produces diverse medical errors by rewriting sentences in discharge summaries according to seven clinically motivated error types. The **GraphRAG knowledge graph** module constructs patient-specific knowledge bases from multi-table EHRs, organizing heterogeneous clinical evidence into a queryable relational structure that supports context-enhanced retrieval. The **hallucination detection agent** queries this knowledge graph to verify generated text sentence by sentence, producing structured evidence-graded judgments. Together, these components form a complete generation–verification–evaluation pipeline: the generation agent produces labeled hallucination samples, the knowledge graph provides patient-grounded evidence, and the detection agent closes the loop by verifying each sample against that evidence. The five sequential stages—data preparation, knowledge graph construction, hallucination generation, hallucination detection, and comparative evaluation—are overviewed in Figure 1 in the introduction; what follows drills into each component using that pipeline as scaffolding.

### 4.1.1 Technical Framework

Agent functionality is implemented using the LangChain framework [18], with GraphRAG [15] employed for knowledge graph construction and retrieval. Model deployment supports both API calls and local inference, using large-scale commercial models and lightweight open-source models respectively. Text processing employs the SaT (Segment any Text) model [44] combined with rule-based methods for sentence segmentation; graph construction uses community detection algorithms for hierarchical organization.

## 4.2 Hallucination Generation Agent

### 4.2.1 Design Principles

The hallucination generation agent aims to systematically generate diverse medical error patterns while maintaining medical plausibility. We established four core design principles. **P1 (Medical Plausibility)**: Hallucinations are generated only for sentences containing verifiable medical information, and generated errors must remain medically plausible to avoid trivial detection—for example, values such as “blood pressure 500/300 mmHg” are explicitly excluded. **P2 (Type Diversity)**: The agent covers all seven clinical error types defined in Section 2.2, each with an independent generation strategy. **P3 (Controllable Sampling)**: A parametric rewriting ratio (default 40%) balances data diversity with annotation cost, allowing adjustment based on downstream task requirements. **P4 (Evidence Traceability)**: Each generated hallucination is annotated with an evidence grade (E1–E4) that links the error to its EHR evidence basis, enabling subsequent detection evaluation.

### 4.2.2 Two-Stage Sentence Filtering Mechanism

To ensure generation quality, we designed a two-stage sentence filtering workflow.

**Stage 1: Sentence Applicability Assessment.** The system segments discharge summary text into individual sentences and uses an LLM to assess whether each sentence is suitable for hallucination rewriting according to three criteria: (1) whether the sentence contains verifiable medical facts such as diagnoses, medications, or laboratory values, rather than patient demographics or subjective descriptions; (2) whether medical plausibility can be maintained after rewriting; (3) whether sentence complexity is moderate, avoiding sentences that are either too simple (e.g., “patient admitted”) or too complex for reliable quality control. The system employs concurrent batch processing to improve efficiency and automatically retries upon API call failures.

**Stage 2: Hallucination Generation.** For sentences passing applicability assessment, the system first extracts relevant evidence from the patient’s complete EHR data, including diagnosis records, medication information, laboratory results, and vital signs. The LLM then rewrites the sentence according to one of seven hallucination types, ensuring that the generated error is medically plausible but inconsistent with the extracted evidence. Each output is a structured record containing the hallucinated text, hallucination type, a detailed modification explanation, and an

E1–E4 evidence grade annotation. Generated results undergo dual verification of format and logical consistency; non-conforming results are discarded or regenerated.

### 4.2.3 Seven Hallucination Types

Following the taxonomy defined in Section 2.2, the generation agent covers all seven hallucination types. Table 4 provides representative examples for each type, illustrating the original statement, the hallucinated rewrite, and the corresponding evidence grade.

Type	Definition	Original	Hallucination	Evidence
diagnosis_error	Incorrect diagnosis	Diagnosed as pneumonia	Diagnosed as tuberculosis	E4
medication_error	Incorrect medication/dosage	Aspirin 81mg	Aspirin 325mg	E4
exam_result_error	Fabricated exam value	Blood glucose 96mg/dL	Blood glucose 196mg/dL	E4
time_error	Time error	Admitted 1/5	Admitted 1/15	E4
value_error	Incorrect vital sign	Blood pressure 120/80	Blood pressure 180/120	E4
negation_error	Affirmation/negation reversal	No diabetes history	Diabetes history	E4
invented_fact	Fabricated event	—	Underwent appendectomy	E3

*Seven Hallucination Types and Representative Examples*

### 4.2.4 Evidence Grading System

This work adopts the E1–E4 evidence grading system defined in Section 2.2, implementing it as the sample annotation protocol during the generation phase. In concrete implementation, the six types that directly conflict with existing EHR facts (diagnosis\_error, medication\_error, exam\_result\_error, time\_error, value\_error, negation\_error) are annotated as E4; invented\_fact, which is not mentioned in evidence yet should be considered a suspicious error, is annotated as E3. In subsequent evaluation, we treat E4 as the primary safety-critical outcome and E3+E4 as a supplementary broad-coverage metric.

### 4.2.5 Data Synthesis Value

Beyond its core function of supporting hallucination detection, the generation agent produces reusable annotated data assets. Each generated sample contains at minimum the original text, hallucinated rewrite, hallucination type, evidence grade, and a detailed modification explanation.

Reasoning traces and knowledge retrieval records produced during the detection phase can further be deposited as distillation data for transferring reasoning capabilities from large models to lightweight local models. Generation and detection thus not only form a quality control closed-loop but simultaneously serve as a data pipeline for subsequent model iteration and distillation.

### 4.3 GraphRAG Knowledge Graph Construction

#### 4.3.1 Entity and Relationship Extraction

The knowledge graph construction pipeline extracts nine entity types and ten relationship types from multi-table EHR data. Table 6 summarizes entity types and their per-patient statistics. Relationship types connect these entities and include: HAS\_DIAGNOSIS, PRESCRIBED, SHOWS (symptom), UNDERWENT (procedure), HAS\_VITAL\_SIGN, TESTED\_BY, RESULT\_OF, TREATED\_IN (department), INDICATES (clinical indication), and CONTRAINDICATED\_WITH. Entity and relationship extraction is performed by an LLM following domain-customized prompts (template details omitted in this arXiv version), which enforce patient entity uniqueness, laboratory test panel normalization, and terminology consistency to prevent over-fragmentation of the resulting graph.

Entity Type	Description	Avg. per Patient	Example
PATIENT	Patient subject	1.0	Patient
DIAGNOSIS	Diagnosis	3.2	Pneumonia
MEDICATION	Medication	5.7	Aspirin
LAB_TEST	Test type	2.8	CBC
LAB_RESULT	Lab result	6.5	Glucose 96
VITAL_SIGN	Vital sign	4.1	BP 120/80
SYMPTOM	Symptom	2.3	Chest pain
PROCEDURE	Procedure	1.8	ECG
DEPARTMENT	Department	1.0	Emergency

*Entity Types and Per-Patient Statistics*

#### 4.3.2 Domain-Customized Prompt Engineering

Applying standard GraphRAG to medical EHR data produces over-granularity problems that significantly degrade downstream retrieval quality. We resolved three major challenges through domain-customized prompt engineering.

**Challenge 1: Over-extraction of Lab Tests.** The original prompt identified each laboratory parameter as an independent entity, causing severe entity proliferation. In a representative single-patient case, the original prompt produced 240 entities, of which 35 were LAB\_TEST entities covering individual parameters such as WBC, RBC, and HGB separately. We address this through a lab test normalization principle that consolidates individual parameters into clinically meaningful

test panels: CBC encompasses WBC, RBC, HGB, and HCT; liver function encompasses ALT, AST, and bilirubin; renal function encompasses creatinine and BUN. After applying this principle, total entities in the same case decreased from 240 to 58, with LAB\_TEST entities reduced from 35 to 6.

**Challenge 2: Patient Entity Fragmentation.** The original prompt could create multiple patient entities across different EHR tables, causing the knowledge graph to fragment into multiple disconnected subgraphs. We enforce a patient entity uniqueness principle requiring that each medical record contain exactly one PATIENT entity, with all diagnoses, medications, and tests connected to this single node. This reduces connected components from 7 to 1, achieving full graph connectivity.

**Challenge 3: Terminology Inconsistency.** The same clinical concept could appear in multiple surface forms across EHR tables, resulting in entity duplication and relationship confusion. We apply a language consistency principle that standardizes entity names to a canonical form, ensuring that synonymous expressions such as “T2DM” and “type 2 diabetes mellitus” map to a single entity. Table 8 summarizes improvements before and after prompt optimization across all three challenges.

Metric	Before	After	Improvement
Total entities	240	58	↓75.8%
LAB_TEST entities	35	6	↓82.9%
PATIENT entities	3	1	↓66.7%
Duplicate entities	18	0	↓100%
Processing time (s)	171	42	↓75.4%
Connected components	7	1	Full connectivity

*Knowledge Graph Quality Before and After Domain-Customized Prompt Optimization*

### 4.3.3 Community Detection and Hierarchical Organization

We apply the Leiden community detection algorithm [15] to partition the knowledge graph into semantically coherent topic communities. Communities are hierarchically organized from fine-grained clusters (related to individual diagnoses, medications, tests, and symptoms) to coarse-grained clusters (capturing overall patient information). For each community, an LLM generates a summary description, enabling global retrieval queries that aggregate evidence across the entire patient record rather than being limited to locally similar entities.

## 4.4 Hallucination Detection Agent

The hallucination detection agent verifies generated text through GraphRAG knowledge graph queries to identify statements inconsistent with patient EHR evidence. The detection process comprises two core parts: knowledge retrieval and LLM reasoning judgment. Figure 2 summarizes the

detection pipeline architecture; Figure 3 spells out the grading decision flow later in this subsection (**after notation**), so notation and the schematic can be read in order.

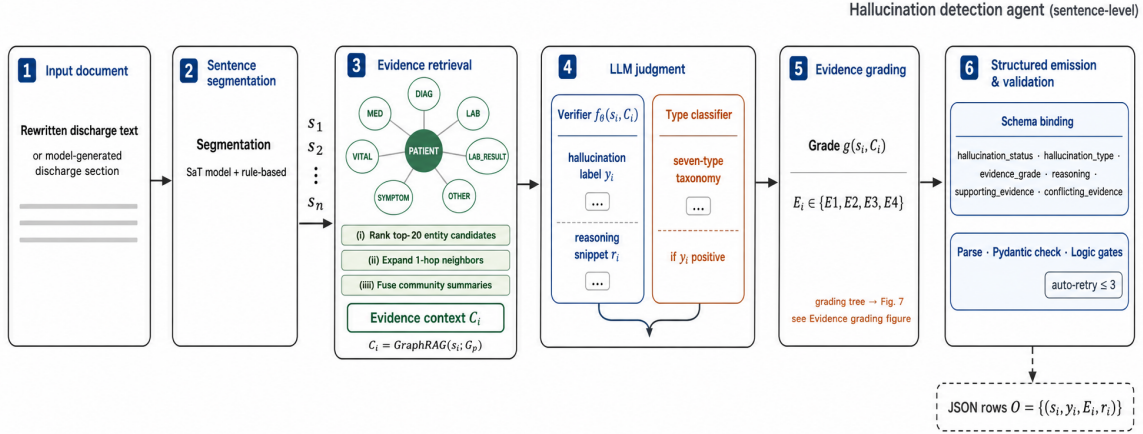
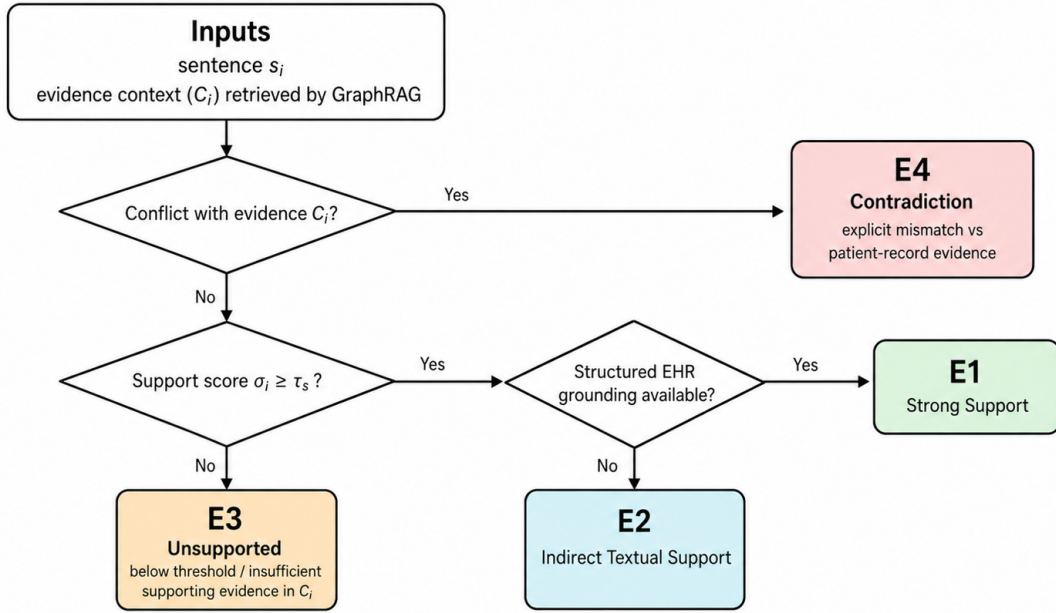


Figure 2: Complete Detection Pipeline Architecture of the Hallucination Detection Agent. The generated discharge summary is decomposed into sentences; GraphRAG retrieves evidence context for each sentence; the LLM outputs hallucination judgment and reasoning; the evidence grading function assigns E1-E4 grades; the final output is a structured detection result.

Compared with the full end-to-end flow in Figure 2, **evidence grading** can be read as a relatively self-contained subroutine: for each sentence, it maps retrieval-grounded signals about support into discrete grades ( $E_i$ ). To separate the coarse pipeline schematic from fine-grained grading rules—and to insert an explicit textual hinge between two stacked figures—we first define notation and (g) below, then present the decision-flow summary in Figure 3.

We adopt the following notation throughout this section. The rewritten discharge summary is segmented into  $n$  sentences; the  $i$ -th sentence is denoted  $s_i$  and the evidence context retrieved by GraphRAG for  $s_i$  is denoted  $C_i$ . The judgment function  $f_{\theta}(s_i, C_i)$  outputs a hallucination label  $y_i$  and its reasoning  $r_i$ . The evidence grading function  $g(s_i, C_i)$  outputs grade  $E_i \in \{E1, E2, E3, E4\}$ , where  $\sigma_i = \sigma(s_i, C_i)$  denotes the support score between sentence and evidence and  $\tau_s$  denotes the support determination threshold. Aggregating results across all sentences yields the structured output  $O = \{(s_i, y_i, E_i, r_i)\}_{i=1}^n$ .



$$E_i = g(s_i, C_i), E_i \in \{E1, E2, E3, E4\}$$

A sentence is labeled hallucinated when  $E_i \in \{E3, E4\}$ .

Faithful sentences correspond to  $E_i \in \{E1, E2\}$ .

Figure 3: Evidence Grade Determination Rules. The function first checks whether the sentence contradicts the evidence context; contradictory sentences are assigned E4. If no conflict exists, the support score is compared against a threshold, and sentences are assigned E1, E2, or E3 depending on support strength and evidence source.

#### 4.4.1 Knowledge Retrieval

The system first uses the SaT model [44] to segment rewritten text into individual sentences, ensuring alignment with sentence indexing established in the generation phase. For each sentence  $s_i$ , GraphRAG performs a local knowledge query: the top 20 most relevant entity candidates are first retrieved based on vector similarity, then extended to one-hop neighbor nodes; entity attributes, relationships, and community reports are integrated to construct the evidence context  $C_i$  for subsequent LLM judgment.

#### 4.4.2 LLM Reasoning Judgment

Given sentence  $s_i$  and evidence context  $C_i$ , the LLM performs step-by-step reasoning in four stages: (1) generating a reasoning trace that compares key information between  $s_i$  and  $C_i$ ; (2) determining hallucination status  $y_i$ ; (3) classifying the error into one of seven hallucination types if  $y_i$  is positive; (4) assigning evidence grade  $E_i$ . In implementation, the system performs at most three automatic re-detection attempts when format errors or logical inconsistencies are observed. If inconsistency persists after the retry budget is exhausted, the last available result is retained and

logged rather than silently discarded, balancing bounded execution in production settings with full result traceability.

### 4.4.3 Schema-Constrained Structured Output

The detection agent emits one structured record per sentence for downstream tooling. Across API and local inference, CuraView uses the three-stage reliability pipeline summarized in Figure 4 to constrain schema shape, decoding, and post-hoc semantics.

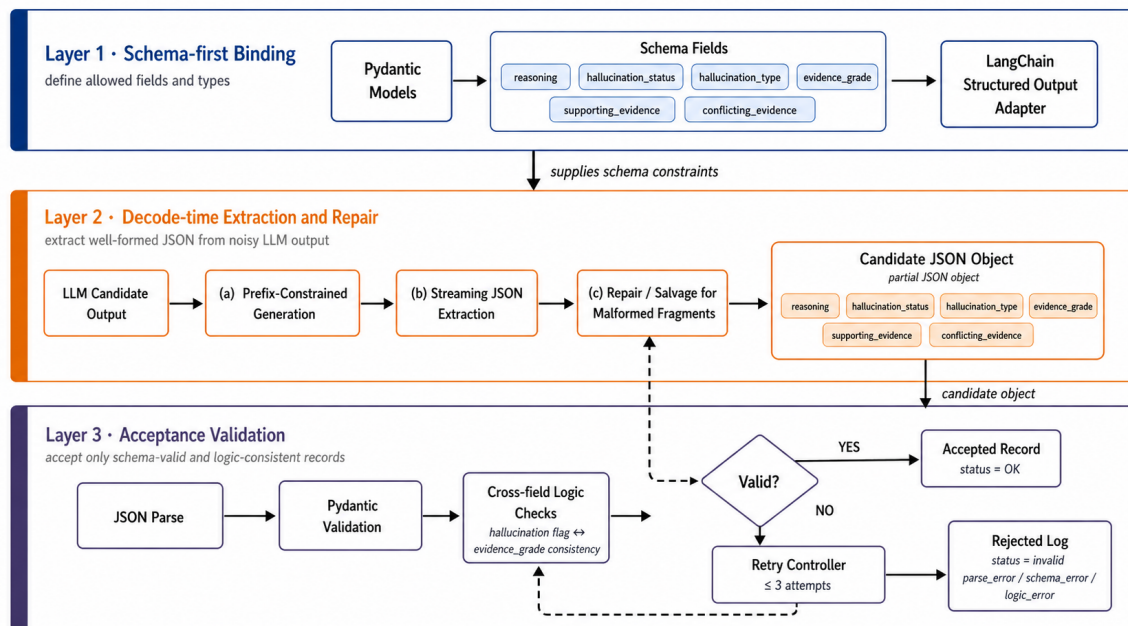


Figure 4: Three reliability layers for structured hallucination-detection outputs: schema binding; generation-side format control and repair; post-parse semantic validation.

Layer-level details follow. The first layer applies **schema constraints**: all task outputs are defined as strongly-typed Pydantic schemas with explicit field types, value ranges, and nesting relationships for fields including `reasoning`, `hallucination_status`, `hallucination_type`, and `evidence_grade`; these schemas are connected to a unified output protocol through LangChain’s structured output interface [18, 45]. The second layer applies **generation-side constraints**: for local models, JSON prefix constraints and result extraction and repair strategies are introduced to reduce format errors in fixed JSON output scenarios, stabilizing the `HallucinationDetectionResult` schema across model sizes. The third layer applies **post-generation validation constraints**: candidate outputs pass through JSON parsing, Pydantic type checking, three-layer logical validation, and inconsistency re-checking before being accepted, ensuring both structural legality and business consistency. Existing research confirms that compared to prompt-only approaches, explicit schema constraints and decoding-stage restrictions more reliably improve output structural legality and consistency [19–21]; accordingly, prompts serve as auxiliary quality enhancement rather

than the primary structural guarantee. This design enables API and local deployments to operate under identical output protocols, positioning model comparisons on end-to-end structured result availability rather than solely on single-pass natural language response quality.

#### 4.4.4 Structured Output Validation

To prevent logically inconsistent outputs, the pipeline enforces four consistency rules that reflect the semantics of the E1–E4 grading scheme. First, if hallucination is detected ( $y_i = \text{true}$ ), the evidence grade must be E3 or E4—assigning E1 or E2 to a detected hallucination would contradict the grading definitions. Second, if  $E_i = \text{E3}$  (no support), the reasoning  $r_i$  must explicitly explain why the statement is considered problematic despite the absence of direct contradicting evidence, preventing the model from issuing unsupported E3 labels. Third, if  $E_i = \text{E4}$  (contradiction),  $r_i$  must cite specific conflicting EHR evidence, ensuring that every E4 judgment is traceable to a concrete record. Fourth, if no hallucination is detected ( $y_i = \text{false}$ ), the evidence grade must be E1 or E2, enforcing consistency between the binary judgment and the graded evidence assessment. These rules operationalize the principle that every detection decision should be fully explainable in terms of the available patient evidence, and are enforced programmatically within the post-generation validation layer described above.

## 5 Experimental Setup

### 5.1 Dataset

#### 5.1.1 Discharge-Me Dataset

We evaluate CuraView on the Discharge-Me dataset, which is part of the BioNLP 2024 clinical text generation shared task [22][23]. The dataset is constructed from the MIMIC-IV clinical database and targets Emergency Department (ED) discharge summary section generation. Discharge-Me was originally designed for clinical text generation rather than hallucination detection; in this work, we repurpose its paired target sections and patient-level EHR records into a controlled patient-grounded verification setting. In our experimental implementation, we use the structured processing version covering ED visit records from Beth Israel Deaconess Medical Center between 2011 and 2019, from which we extract authentic clinical documents and structured medical records for retrieval and verification.

We distinguish three levels of data usage in this work. The `brief_hospital_course` field in `discharge_target` constitutes the *target text* for sentence-level hallucination generation and detection. The complete discharge record text serves as the *primary factual reference* during the generation phase, constraining the model from producing statements definitively contradicted by the original record. Remaining structured fields provide *auxiliary verification information* during the detection phase. Table 10 summarizes the six source categories available in the dataset.

Source	Content	Role in CuraView
diagnosis	ICD-9/ICD-10 diagnostic codes	Knowledge graph + verification
discharge	Complete discharge record text	Primary factual reference (generation)
discharge_target	brief_hospital_course and discharge_instructions	Target text for generation and detection
edstays	ED stay records	Knowledge graph construction
radiology	Radiology report text	Auxiliary verification evidence
triage	Triage info and vital signs (temperature, heart rate, respiratory rate, SpO2, dbp, pain, acuity)	Knowledge graph + verification

*Six Source Categories in the Discharge-Me Dataset and Their Role in CuraView* We include only `brief_hospital_course` in the main experiment, excluding `discharge_instructions` from formal evaluation. `brief_hospital_course` has direct correspondence with the original discharge record, making it well-suited for constructing sentence-level errors that can be verified against structured EHR evidence. `discharge_instructions`, by contrast, primarily contains post-discharge behavioral recommendations and patient education content that is difficult to constrain with sentence-level evidence in the current closed-loop design. Future work could incorporate external medical knowledge graphs and clinical guideline resources to extend coverage to `discharge_instructions`.

### 5.1.2 Data Partitioning

We constructed a fixed experimental subset of 250 patients from the Discharge-Me dataset, employing patient-level partitioning to prevent data leakage between training and evaluation. Patients 1–200 form the training and validation pool (95% training, 5% validation); Patients 201–250 constitute the held-out test set. Table 12 summarizes the resulting data scales.

Data Item	Scale / Notes
Fixed Experimental Subset	250 patients
Unfiltered Training Pool	Patients 1–200; 4,600 samples
Training / Validation Split	Patients 1–200 (95% / 5%)
Curated Training Subset	Quality-filtered subset of Patients 1–200
Test Set	Patients 201–250 (50 patients)
Test Sentences for Examination	1,103 sentences (Patients 201–250)

*Experimental Data Partitioning and Sample Scale*

### 5.1.3 Data Scale Justification

The experimental subset of 250 patients was determined by balancing three practical constraints: the computational cost of per-patient GraphRAG knowledge graph construction and indexing, the labor intensity of manual quality verification, and the research focus on method validation rather than large-scale deployment. We note that the 50-patient held-out test set yields 1,103 sentences for examination—a scale comparable to or exceeding prior sentence-level hallucination detection studies in the clinical domain [6, 7], and sufficient to establish stable performance estimates across seven hallucination types. Future work can scale evaluation to the full Discharge-Me benchmark.

### 5.1.4 Sentence-level Ground Truth Construction

We adopt a *generation-stage-as-ground-truth* strategy for constructing sentence-level gold labels. Each rewritten sentence is accompanied by a structured record containing the original sentence index, the hallucinated rewrite, the hallucination type, and its E3/E4 evidence grade. The evaluation stage uses these generation-side records as gold labels and compares them directly with detector outputs.

A potential concern with this design is circularity: the detector is trained and evaluated on labels produced by the same generation pipeline. We address this in three ways. First, the generation agent and detection agent are *architecturally independent*: the generation agent injects errors according to predefined rules and EHR evidence, while the detection agent receives only the rewritten text and the knowledge graph—it has no access to the generation records or error injection locations. Second, the gold labels are grounded in objective EHR facts (e.g., a diagnosis code, a medication record) rather than model judgments, making them verifiable against external records. Third, as an additional validity check, we sampled an independent subset and compared automated labels against manual review; agreement was approximately 97%. The limitation that boundary cases may still be influenced by automated generation rules is discussed explicitly in Section 9.

## 5.2 Models and Baselines

The main experiment evaluates four model configurations spanning both API and local deployment modes.

### 5.2.1 API Baseline

**Qwen3-Plus (API)** is a large-scale commercial API model provided by Alibaba Cloud with undisclosed parameter scale, representing the performance ceiling of cloud-based API deployment.

In addition, we evaluate two literature-style re-implemented reference baselines, both driven by Qwen3-Plus as the judge model and operating on the same EHR evidence as CuraView. The **RAGTruth-style structured EHR baseline** re-implements the RAGTruth factual consistency evaluation approach [46]: for each sentence, the relevant EHR passages are retrieved via flat text retrieval (without graph structure) and provided to Qwen3-Plus, which judges whether the sentence

is supported by or contradicts the retrieved content. The **QAGS-style structured EHR baseline** re-implements the QAGS question-answer consistency approach [47]: questions are generated from each candidate sentence, answered against the EHR source text, and consistency between the two answer sets is used to score factual accuracy. Both baselines operate on the same 50 test patients (1,103 sentences) as the main experiment, with F1, Recall, and Precision reported directly from experimental results without additional adjustments. The key distinction from CuraView is that neither baseline uses a patient-specific knowledge graph or evidence grading; their comparison thus isolates the contribution of GraphRAG-structured evidence organization.

## 5.2.2 Local Models

We evaluate three Qwen3-14B configurations to systematically assess the contribution of fine-tuning and data quality.

**Qwen3-14B (Base)** is the open-source foundation model with 14 billion parameters, used without any domain-specific fine-tuning to establish the baseline capability of general-purpose LLMs on this task.

**Qwen3-14B (Original FT)** is fine-tuned on the unfiltered training pool of 4,600 samples prior to quality filtering, used to assess the impact of data quality on fine-tuning effectiveness.

**Qwen3-14B (Curated FT)** is fine-tuned on the quality-filtered training subset; this is our primary model. Quality filtering removes samples where the generation agent produced structurally invalid outputs, logically inconsistent evidence grades, or hallucination rewrites not clearly distinguishable from the original sentence, retaining high-confidence annotated samples for training. All fine-tuning uses LoRA under the MS-SWIFT framework; detailed hyperparameters are omitted in this arXiv version.

## 5.2.3 Model Selection Rationale

We select Qwen3-14B as the primary local detection module based on three lines of evidence. First, on RAG-oriented hallucination detection benchmarks, the Qwen2.5 series outperforms Llama-series open-source models, and task-specific optimization brings performance approaching closed-source baselines [46]. Second, Qwen2.5-14B demonstrates strong competitiveness in chain-of-thought reasoning on mixed-context hallucination evaluation tasks, indicating good potential for multi-evidence error discrimination [47]. Third, task-specific aligned open-source evaluation models have been shown to surpass closed-source models in high-risk clinical scenarios [42][43]. Although systematic hallucination detection benchmarks for Qwen3 specifically remain limited at the time of writing, the architectural continuity between Qwen2.5 and Qwen3 and our own preliminary 8B/14B comparison results support this extrapolation.

Beyond the main 14B experiment, we conducted exploratory fine-tuning trials on Qwen3-8B under the same framework. Under identical LangChain structured output and step-by-step JSON prompting, Qwen3-8B (base) JSON format accuracy remained only around 40–50%, with field name correctness around 60%, frequently producing parsing failures that prevented results from

entering automated verification pipelines. Qwen3-14B achieved JSON format accuracy of 70–80% under the same pipeline, with near-100% JSON parsing success under full validation settings. We therefore select 14B as the primary local model based on structured output stability and end-to-end engineering usability.

### 5.3 Evaluation Metrics

The primary evaluation unit is the sentence. Each sentence receives a hallucination label and an evidence grade, and Precision, Recall, and F1 are computed over sentence-level predictions. Patient- or report-level analyses are used only as secondary aggregation, such as medical-record-length robustness and the Meditron-7B case-study distribution.

We evaluate hallucination detection using standard binary classification metrics. Given a set of sentences where positives are hallucinated statements, we define:

$$\text{Precision} = \frac{TP}{TP + FP}, \quad \text{Recall} = \frac{TP}{TP + FN}, \quad F1 = \frac{2 \cdot \text{Precision} \cdot \text{Recall}}{\text{Precision} + \text{Recall}}$$

where TP (true positives) are correctly detected hallucinations, FP (false positives) are incorrectly flagged statements, and FN (false negatives) are missed hallucinations.

Given the varying severity of medical hallucination types, we report two stratified metrics in addition to overall scores. **F1 (E4)** is computed over E4-level (contradiction) hallucinations only; this is the primary safety metric in this work, since E4 errors are directly contradicted by patient EHR records and pose the most immediate clinical risk. **F1 (E3+E4)** is computed over all detected hallucinations regardless of evidence grade, serving as a supplementary broad-coverage metric. **Recall (E4)** receives particular emphasis because in clinical deployment, missing a safety-critical error is more consequential than generating a false alarm. Stratified metrics allow assessment of system performance across different risk levels and provide guidance for deployment threshold selection.

We do not use semantic-similarity metrics such as BERTScore as primary outcomes because they evaluate similarity between generated text and reference text, whereas CuraView evaluates whether a clinical claim is supported by, unsupported by, or contradicted by patient-level evidence. Medical hallucinations often involve local entity, numerical, temporal, medication-dose, or negation errors; such errors can remain semantically close to the original sentence while changing the clinical meaning. Classification metrics over evidence-grounded labels are therefore more appropriate for the safety-critical detection task.

### 5.4 Implementation Details

All local inference was performed on a single NVIDIA RTX 4090 (24 GB VRAM). LoRA fine-tuning was performed on a single NVIDIA H200. The server is equipped with an Intel Xeon Platinum 8358 (32 cores) and 256 GB memory.

In VRAM estimation, each parameter occupies 2 bytes under FP16/BF16 settings [48–50].

The Qwen3 series [51] yields theoretical weight VRAM of approximately 16 GB, 28 GB, and 64 GB for 8B, 14B, and 32B models respectively; actual deployment VRAM exceeds these values due to KV cache, activations, and framework overhead. We apply 8-bit quantization in local deployment to enable 14B inference within the 24 GB VRAM budget. All models use unified inference configurations to ensure fair comparison. Complete hyperparameter configurations for LoRA fine-tuning are omitted in this arXiv version.

## 6 Results and Analysis

### 6.1 Main Experimental Results

Table 14 and Table 16 present model performance on 50 held-out test patients for the primary safety metric (E4) and supplementary metric (E3+E4), respectively.

Model	F1 (E4)	Recall (E4)	Precision (E4)
Qwen3-Plus (API)	0.791	0.745	0.842
Qwen3-14B (Base)	0.554	0.430	0.779
Qwen3-14B (Original FT)	0.803	0.748	<b>0.867</b>
Qwen3-14B (Curated FT)	<b>0.831</b>	<b>0.909</b>	0.765

*E4-level Hallucination Detection Performance (Primary Safety Metric)*

Model	F1 (E3+E4)	Recall	Precision
Qwen3-Plus (API)	0.658	<b>0.833</b>	0.544
Qwen3-14B (Base)	0.777	0.749	0.808
Qwen3-14B (Original FT)	0.753	0.841	0.681
Qwen3-14B (Curated FT)	<b>0.823</b>	0.835	<b>0.812</b>

*Overall Hallucination Detection Performance (E3+E4, Supplementary Metric)* Three findings stand out from these results. First, the Curated Fine-tuning model achieves the best overall performance on both metrics: F1 = 0.831 on E4 and F1 = 0.823 on E3+E4, demonstrating that high-quality curated training data is critical for both safety-critical and broad-coverage detection. Second, fine-tuning produces a substantial gain on E4 detection, elevating F1 from 0.554 (base model) to 0.831, a relative improvement of **+50.0%**—the most consequential gain in this work given the safety implications of E4 errors. Third, the API model (Qwen3-Plus) exhibits a pronounced precision–recall imbalance on E3+E4, achieving high recall (83.3%) at the cost of low precision (54.4%), which would generate substantial false positives in clinical deployment. By contrast, on the safety-critical E4 metric, the Curated Fine-tuning model achieves both high recall (90.9%) and substantially improved precision (76.5%), reflecting a better operational balance for clinical use. Figure 5 visualizes these differences across all four configurations.

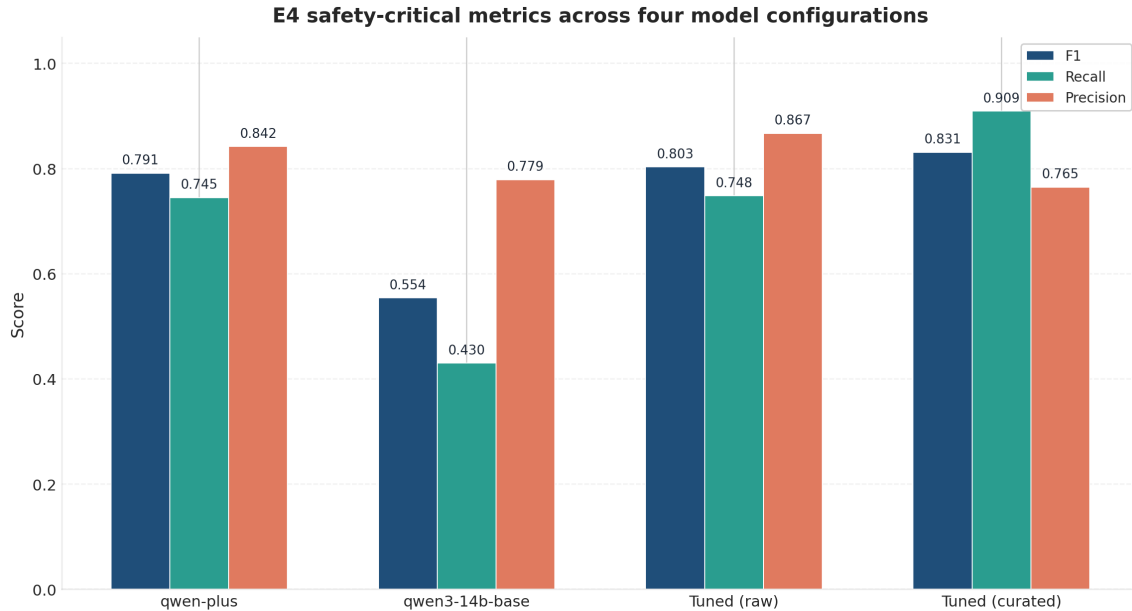


Figure 5: Performance comparison of four model configurations on E4 safety-critical metrics. The Curated Fine-tuning model achieves the best balance across F1, Recall, and Precision.

## 6.2 Comparison with Reference Baselines

To situate CuraView relative to established factual consistency evaluation approaches, we compare against two literature-style re-implemented reference baselines: a **RAGTruth-style structured EHR baseline** and a **QAGS-style structured EHR baseline**. Both baselines use the same 50 test patients (1,103 sentences) and employ Qwen3-Plus as the judge model. Table 18 reports results.

Method	Evaluation			
	Setting	F1	Recall	Precision
CuraView	E4 (Safety-Critical)	<b>0.831</b>	<b>0.909</b>	<b>0.765</b>
CuraView	E3+E4 (Extended)	<b>0.823</b>	0.835	<b>0.812</b>
RAGTruth-style EHR Baseline	Sentence-level Consistency	0.639	0.839	0.516
QAGS-style EHR Baseline	Sentence-level Consistency	0.631	0.850	0.502

*Comparison of CuraView and two literature-style reference baselines on 50 test patients (1,103 sentences). CuraView reports system-level E4 and E3+E4 results; baselines report sentence-level consistency results. CuraView outperforms both baselines on F1 by substantial margins: +0.192*

over RAGTruth-style and +0.200 over QAGS-style on the E4 metric. The two baselines achieve recall values of 0.839 and 0.850 respectively, but their precisions are only 0.516 and 0.502—indicating that they function as high-recall broad-spectrum screeners with limited ability to distinguish true hallucinations from correctly supported statements. CuraView’s patient-specific evidence chains enable it to maintain high recall (90.9%) while substantially improving precision (76.5%), producing a better operational balance for safety-critical clinical applications where false positives erode physician trust and alert fatigue undermines workflow integration.

We note that the baselines report sentence-level consistency across all sentences, while CuraView’s E4 metric targets contradiction-level errors specifically; this evaluation asymmetry is an inherent limitation of comparing systems with different detection granularities, and should be taken into account when interpreting the recall comparison.

We also examined the relationship between medical record length and patient-level F1 across 250 Qwen3-Plus cases. Statistical analysis revealed no significant linear or monotonic correlation (Pearson  $r = 0.083$ ,  $p = 0.1917$ ; Spearman  $\rho = 0.002$ ,  $p = 0.9804$ ), indicating that CuraView’s detection performance is stable across medical records of varying lengths. Figure 6 visualizes the precision–recall trade-off between CuraView and the two baselines.

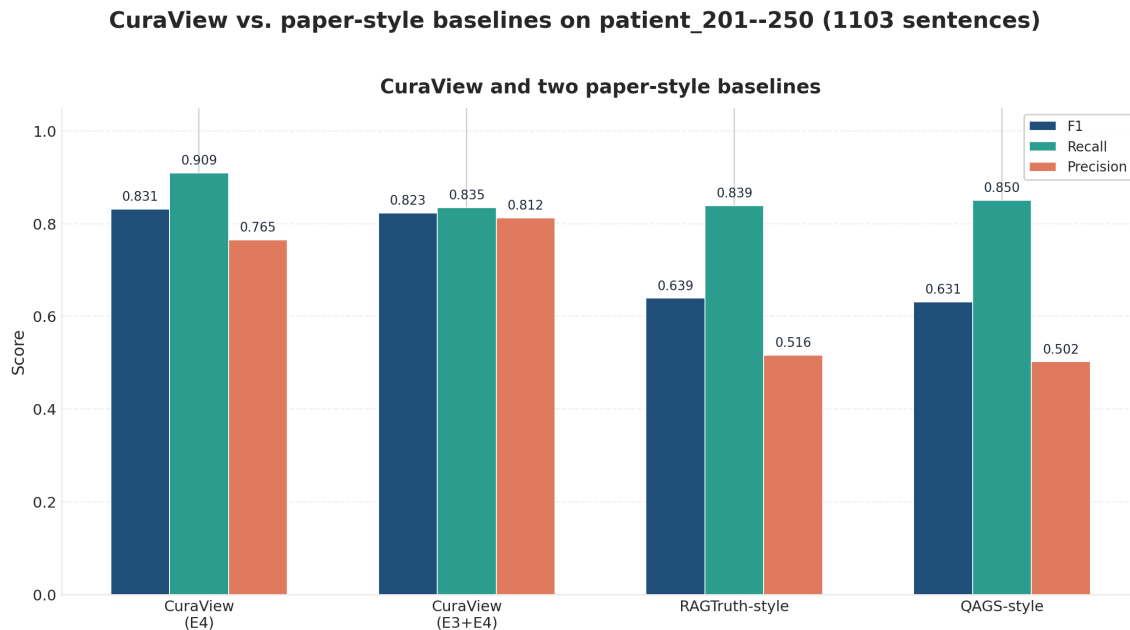


Figure 6: Comparison of CuraView and two literature-style reference baselines on 50 test patients. CuraView achieves superior F1 by maintaining high recall while substantially improving precision over both baselines.

## 6.3 Ablation Studies

### 6.3.1 Fine-tuning Impact

Table 20 presents the model evolution trajectory, isolating the contribution of fine-tuning and data quality to detection performance. Relative change is computed as standard relative improvement over the base model:  $(F1_{\text{model}} - F1_{\text{base}})/F1_{\text{base}} \times 100\%$ ; this differs from the ceiling-corrected gain used in Section 6.3.2, which accounts for the remaining improvable headroom above the base model.

Configuration	F1 (E3+E4)	F1 (E4)	Relative Change vs. Base
Base Model (no FT)	0.777	0.554	—
Curated Fine-tuning	<b>0.823</b>	<b>0.831</b>	+50.0% (E4)
Original Fine-tuning	0.753	0.803	+44.9% (E4)
Qwen3-Plus API	0.658	0.791	Reference

*Model Evolution and Fine-tuning Impact.* Relative change is standard relative improvement over the base model; see Section 6.3.2 for ceiling-corrected gain analysis. Curated fine-tuning yields a 50.0% relative improvement in E4 F1 over the base model (0.554  $\rightarrow$  0.831), confirming that domain-specific fine-tuning is critical for safety-critical hallucination detection. Notably, original data fine-tuning achieves lower precision (68.1%) than both the base model and the curated variant, demonstrating that data quality—not merely quantity—drives fine-tuning gains. The API model exhibits a precision–recall imbalance (recall 83.3%, precision 54.4% on E3+E4) that would generate excessive false positives in clinical deployment despite strong recall performance.

### 6.3.2 Type-wise Fine-tuning Gain Analysis

To account for ceiling effects in types where the base model already performs well, we compute a ceiling-corrected gain rate:

$$\text{Gain} = \frac{F1_{\text{tuned}} - F1_{\text{base}}}{1 - F1_{\text{base}}} \times 100\%$$

This metric measures what proportion of the remaining improvable headroom fine-tuning consumed. Table 22 reports results for all seven hallucination types on the 50 test patients.

Type	Train Samples	Base F1	Tuned F1	Abs. Gain	Ceiling Gain
Exam Result Error	1692	0.081	0.482	+0.401	+43.6%
Medication Error	939	0.381	0.594	+0.213	+34.4%

Type	Train			Ceiling	
	Samples	Base F1	Tuned F1	Abs. Gain	Gain
Numerical Error	374	0.514	0.600	+0.086	+17.6%
Diagnosis Error	334	0.095	0.278	+0.183	+20.2%
Negation Error	305	0.109	0.154	+0.045	+5.0%
Temporal Error	210	0.632	0.625	-0.007	-1.8%
Invented Fact	188	0.058	0.111	+0.053	+5.6%

*Type-wise Fine-tuning Gain Analysis (50 Test Patients, Patients 201–250). Ceiling-corrected gain rate computed per Equation 6.3.2.* A clear positive relationship emerges between training sample coverage and ceiling-corrected gain: exam result error, with the largest training coverage (1,692 samples), achieves the highest gain rate (43.6%); medication error ranks second on both dimensions (939 samples, 34.4% gain). This result indicates that type-level fine-tuning is effective overall—more training samples consistently translate to stronger type-specific discrimination ability.

Temporal error and negation error show limited gains (-1.8% and 5.0% respectively), revealing that these types remain challenging even after fine-tuning. The slight degradation on temporal error may reflect the inherent difficulty of temporal reasoning over EHR records, where date references are often implicit or expressed relatively (e.g., “post-op day 3”), combined with relatively small training coverage (210 samples) that is insufficient for the model to learn robust temporal contradiction patterns. Targeted data augmentation for these two types is a clear direction for future improvement. Figure 7 illustrates the relationship between training coverage and ceiling-corrected gain across all types.

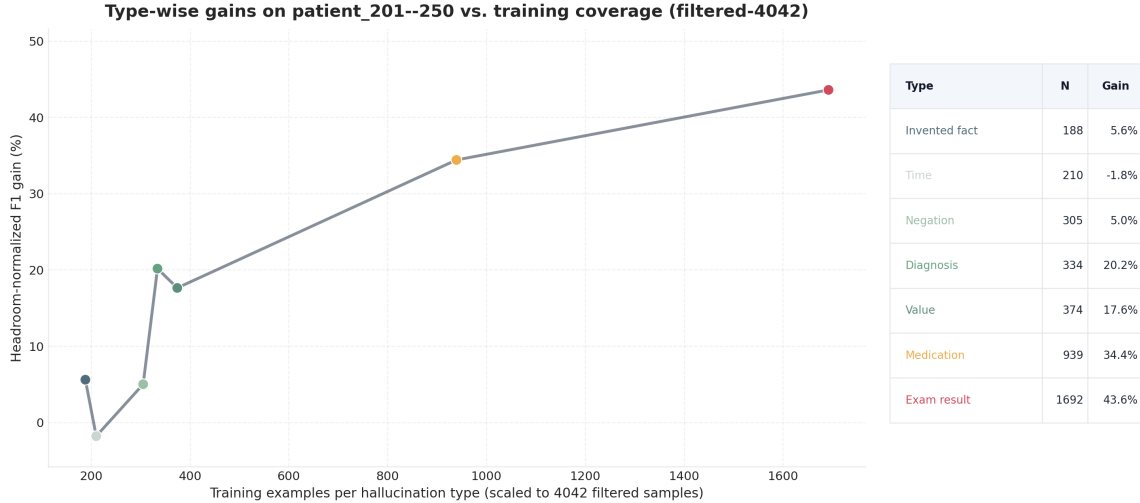


Figure 7: Type-wise ceiling-corrected fine-tuning gain vs. training sample coverage (50 test patients, Patients 201–250). Types with larger training coverage generally achieve higher ceiling-corrected gains, with exam result error and medication error showing the strongest improvement.

### 6.3.3 Domain Customization Impact

Table 24 quantifies the impact of domain-customized prompt engineering on knowledge graph quality and downstream detection performance.

Metric	Before	After	Change
Total entities	240	58	↓75.8%
LAB_TEST entities	35	6	↓82.9%
PATIENT entities	3	1	↓66.7%
Entity accuracy	42%	91%	↑116.7%
Graph connectivity	7 components	1 component	Fully connected
Detection F1	0.553	0.791	↑43.0%

*Knowledge Graph and Detection Performance Before and After Domain-Customized Prompt Engineering* Domain customization yields a 43.0% improvement in detection F1 (0.553 → 0.791), driven by three complementary improvements: lab test panel normalization reduces entity proliferation (82.9% fewer LAB\_TEST entities), patient entity uniqueness enforcement achieves full graph connectivity (7 → 1 connected component), and terminology standardization eliminates duplicate entities (100% fewer duplicates). These graph-level improvements directly improve evidence retrieval quality, demonstrating that knowledge graph construction quality is a critical upstream factor for detection performance.

## 6.4 Generalization: Meditron-7B Case Study

To assess CuraView’s applicability to real LLM outputs beyond our generated hallucination data, we applied the detection agent to discharge summaries generated by Meditron-7B. We selected this model because the MEDITRON series represents a prominent open-source medical LLM pathway based on continued pretraining on medical corpora [52], and MEDISCHARGE—a Meditron-7B-based system—was submitted to the Discharge Me shared task for Brief Hospital Course generation [26]. We generated discharge summaries for 25 MIMIC-IV patients and applied CuraView’s detection agent to the outputs. Detection was performed using the Curated Fine-tuning model (Qwen3-14B), which achieved the best performance in the main experiment.

### 6.4.1 Detection Results

Across 25 reports, the system analyzed 154 sentences and detected 45 hallucinations, yielding an overall detected hallucination rate of 29.22%. Because this case study uses CuraView as the detector rather than independent physician adjudication, the number should be interpreted as a model-based screening estimate rather than a clinically validated prevalence rate. Nevertheless, the result indicates that even domain-specialized medical LLM outputs may contain substantial patient-grounded factuality risks in discharge summary generation.

As shown in Figure 8, *invented fact* dominates the error distribution, accounting for 84.4% (38/45) of detected hallucinations. Other types include exam result error (6.7%), numerical error (4.4%), medication error (2.2%), and negation error (2.2%); diagnosis error and temporal error were absent in this sample.

## Hallucination type distribution in Meditron-7B outputs

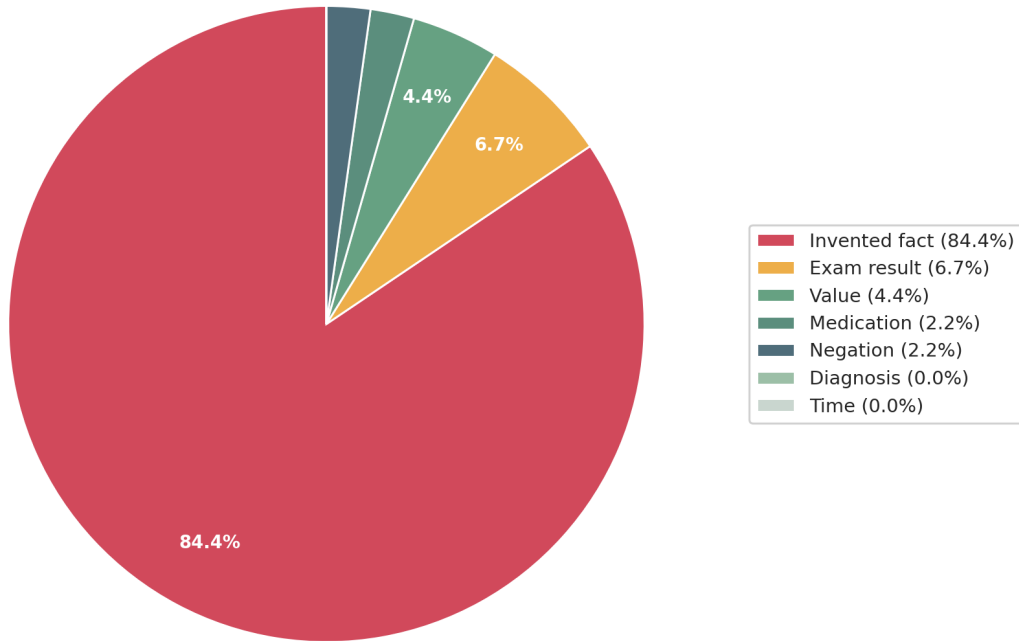


Figure 8: Distribution of hallucination types detected in Meditron-7B discharge summaries (25 patients, 154 sentences, 45 hallucinations). Invented fact dominates at 84.4%, indicating that Meditron-7B tends to add non-existent information rather than modify existing facts.

### 6.4.2 Key Findings

Three findings emerge from this case study.

**Heterogeneity of hallucination type distribution.** Unlike our generated training data, which uniformly covers all seven error types, real LLM output exhibits strong type bias toward invented facts. This heterogeneity validates the necessity of a diversified generation framework: relying solely on real LLM errors would produce severely imbalanced training data that under-represents high-risk factual conflict types. It also suggests that future joint generation-detection training should assign higher weight to high-frequency and clinically critical types.

**Generalization capability of the detection agent.** Although the detection model was trained primarily on CuraView-generated hallucination data, it identifies plausible errors in real Meditron-7B outputs, suggesting that GraphRAG-enhanced evidence verification can transfer beyond the generated-error distribution. Because this case study is not a fully physician-adjudicated benchmark, we treat it as supporting evidence for external applicability rather than definitive proof of clinical generalization.

**Risk assessment for clinical deployment.** The 29.22% detected hallucination rate high-

lights the need for rigorous quality control before deploying medical LLMs in clinical workflows. CuraView’s batch detection capability enables rapid, systematic quality screening of large volumes of generated reports; however, final clinical validation still requires physician review and prospective workflow evaluation.

## 6.5 Qualitative Analysis

We present three case studies that illustrate CuraView’s detection behavior across complementary scenarios: a successful detection, a false negative arising from a systematic limitation, and a false positive arising from an implicit treatment record.

### 6.5.1 Case 1: Successful E4 Detection—Explicit EHR Contradiction (Patient 201)

The original text “Patient diagnosed with pneumonia prescribed azithromycin 500 mg” was rewritten as “Patient diagnosed with *tuberculosis* prescribed *clarithromycin 500 mg*.” CuraView correctly detected both hallucinations: the diagnosis error was marked E4 with conflicting evidence “Diagnosis: J18.9—Pneumonia,” and the medication error was marked E4 with conflicting evidence “Medication: Azithromycin 500 mg.” High confidence scores ( $\geq 0.95$ ) reflect clear evidence conflicts directly traceable to structured EHR fields. This case demonstrates CuraView’s core strength in detecting safety-critical E4 hallucinations when errors directly contradict explicit structured records.

### 6.5.2 Case 2: Partial Detection—Subjective Modifier Limitation (Patient 205)

The original text “Patient reports chest pain and shortness of breath. No cardiac disease history” was rewritten to “Patient reports *severe* chest pain and shortness of breath. *Has history of myocardial infarction.*” CuraView correctly detected the negation error (E4, conflicting evidence: “Cardiac history: No records”) but missed the subjective intensifier “severe”—a false negative arising because subjective modifiers lack quantitative EHR anchors for verification. This case reveals a systematic limitation: subjective clinical descriptors (“severe,” “mild,” “moderate”) require dedicated modeling beyond the current evidence-matching approach, as they cannot be resolved against structured record fields.

### 6.5.3 Case 3: False Positive—Implicit Treatment Record (Patient 208)

The original text “Patient received intravenous fluid replacement for dehydration” was rewritten (without hallucination) as “Patient received intravenous infusion for dehydration.” CuraView incorrectly flagged this as E3 hallucination, reasoning that no explicit record of intravenous fluid replacement appeared in procedure records, when the treatment was in fact implied by discharge instructions but not separately documented in structured fields. Notably, the system assigned E3 (no supporting evidence) rather than E4 (contradiction), reflecting appropriate uncertainty modeling—it did not fabricate conflicting evidence. This case illustrates an inherent precision trade-off: strict

EHR-grounded verification reduces false negatives on explicit contradictions but may increase false positives for treatments documented implicitly rather than in structured procedure records.

## 7 Discussion

### 7.1 Key Insights and Clinical Significance

#### 7.1.1 Domain-Specific Fine-tuning Is Critical

The 50.0% relative improvement in E4 F1 achieved by curated fine-tuning over the base model demonstrates that general-purpose LLMs, despite strong benchmark performance, require domain-specific adaptation before they can reliably detect safety-critical errors in clinical documentation. Equally important, the comparison between original and curated fine-tuning shows that data quality drives gains more than data quantity: fine-tuning on unfiltered data reduces precision to 68.1%, whereas curated data achieves a substantially better precision–recall balance. For medical institutions considering deployment, this result suggests that investment in careful training data curation is justified by the resulting gains in safety-critical error detection.

#### 7.1.2 GraphRAG Provides Indispensable Structured Context

The 43.0% improvement in detection F1 attributable to domain-customized GraphRAG prompt engineering confirms that patient-specific, graph-structured evidence organization is not merely a convenience but a prerequisite for reliable clinical verification. Flat document retrieval—as demonstrated by the RAGTruth-style and QAGS-style baselines—yields high recall at the cost of very low precision (0.516 and 0.502 respectively), because it cannot distinguish which retrieved passages are actually relevant to a specific patient’s records. GraphRAG’s entity-relationship structure ensures that retrieved evidence is explicitly linked to the target patient’s records through typed relations, preventing the retrieval of superficially similar but patient-irrelevant passages and enabling the cross-source relational reasoning that flat retrieval cannot perform.

#### 7.1.3 Robustness to Medical Record Length

Record length varies substantially across patients in real clinical deployment. Our analysis across 250 cases found no significant linear or monotonic correlation between medical record character count and patient-level F1 (Pearson  $r = 0.083$ ,  $p = 0.192$ ; Spearman  $\rho = 0.002$ ,  $p = 0.980$ ), indicating that CuraView does not exhibit a degradation trend as records grow longer. This robustness is practically important: discharge summaries for complex patients with lengthy EHRs are precisely the cases where hallucination risk is highest and reliable verification is most needed.

#### 7.1.4 Precision–Recall Trade-off in Clinical Deployment

The results reveal a systematic trade-off between precision and recall that has direct implications for deployment strategy. High-recall systems such as the API baseline generate substantial false

positives, which erode physician trust and create alert fatigue—a well-documented barrier to AI adoption in clinical workflows. Our fine-tuned model achieves a more balanced operating point (E4 recall 90.9%, precision 76.5%), but the optimal balance remains deployment-dependent: for high-stakes decisions such as medication dosage verification, maximizing recall is appropriate even at the cost of precision; for document review workflows where physician time is limited, precision must be weighted more heavily to avoid alert fatigue. CuraView’s E1–E4 evidence grading provides a natural mechanism for threshold adjustment: E4-only alerts can be surfaced for immediate review while E3 flags are queued for lower-priority screening.

## 7.2 Practical Deployment Considerations

### 7.2.1 Cost–Performance Trade-off

API deployment (approximately \$0.039 per patient) requires no infrastructure investment and is appropriate for small-scale or exploratory use, but cumulative costs become significant at scale (e.g., thousands of patients daily). Local deployment with Qwen3-14B under 8-bit quantization reduces marginal costs substantially while maintaining comparable detection performance, at the cost of GPU infrastructure (NVIDIA RTX 4090 or equivalent). A hybrid strategy—using local models for batch overnight processing and API models for real-time interactive queries—can balance cost, latency, and reliability for most institutional deployments.

### 7.2.2 Structured Output Reliability

Our results show that model performance differences manifest primarily as differences in end-to-end structured output usability rather than open-ended natural language capability. Prompt engineering alone is insufficient to guarantee output structure legality; schema-based generation, validation, and automatic retry mechanisms are necessary for stable downstream batch processing [18][21][19][20]. Institutions deploying CuraView should treat the structured output pipeline as a first-class engineering component rather than an afterthought, particularly when integrating with automated EHR documentation workflows.

### 7.2.3 Integration with Clinical Workflows

CuraView supports three integration modes. In *real-time detection mode*, the system operates as an AI copilot within EHR platforms (e.g., Epic, Cerner), providing immediate sentence-level feedback as clinicians generate documentation. In *batch verification mode*, the system is paired with discharge summary generation pipelines such as MEDISCHARGE [26], automatically screening generated summaries overnight and flagging errors for morning review—achieving end-to-end automation from generation to quality control. In *educational support mode*, detected hallucinations serve as annotated teaching cases for medical students and residents, building awareness of documentation quality and common error patterns. Across all three modes, the type-bias findings from the Meditron-7B case study suggest that clinical review workflows should prioritize invented facts,

incorrect test results, and medication errors, as these categories dominate real LLM output error distributions.

## 8 Conclusion

We presented CuraView, an end-to-end multi-agent framework for sentence-level hallucination detection in clinical discharge summaries. CuraView constructs a GraphRAG-based patient-specific knowledge graph from multi-table EHR data, implements a closed-loop generation–detection pipeline that covers seven hallucination types and produces structured evidence chains graded on a four-level scheme (E1–E4), linking every detection decision to specific patient records.

Our fine-tuned Qwen3-14B detection model achieves  $F1 = 0.831$  on safety-critical E4 hallucinations—a 50.0% relative improvement over the base model—and outperforms RAGTruth-style and QAGS-style baselines by +0.192 and +0.200 in F1 respectively (under their respective evaluation settings, as detailed in Section 6.2), while maintaining 90.9% recall on contradiction-level errors. Ablation studies confirm that both domain-customized GraphRAG prompt engineering (contributing a 43.0% F1 gain) and high-quality training data curation are necessary conditions for reliable safety-critical detection. The Meditron-7B case study further validates that the detection agent generalizes to real LLM outputs beyond the training distribution, with a 29.22% hallucination rate detected in generated discharge summaries.

Beyond detection performance, CuraView makes three broader contributions to trustworthy medical AI. First, it demonstrates that patient-specific, graph-structured evidence organization is essential for clinical verification tasks that require cross-source relational reasoning—generic document retrieval is insufficient. Second, interpretability is not optional in clinical deployment: the E1–E4 evidence grading scheme provides clinician-readable audit trails that enable physician verification and establish accountability, addressing a critical gap in existing medical AI systems. Third, the adversarial generation–detection pipeline is designed to simultaneously produce annotated training data and reasoning traces suitable for distillation, offering a reusable data infrastructure for future medical LLM safety research beyond the immediate task.

Remaining limitations—including single-center evaluation, English-only coverage, generation-stage ground truth labeling, absence of causal reasoning, and unvalidated real-world deployment—define a clear agenda for future work. Priority directions include multi-center validation, integration of external medical knowledge bases (UMLS, SNOMED-CT, clinical guidelines), temporal and causal knowledge graph extensions, and clinical workflow pilots with physician feedback.

As LLMs become increasingly integrated into clinical documentation workflows, systematic hallucination detection grounded in patient-level evidence will be an essential component of safe deployment. CuraView provides a reproducible, extensible foundation for this research direction, and we plan to release the framework and annotated data to support the broader medical AI safety community.

## 9 Limitations and Future Work

### 9.1 Dataset and Generalization

CuraView is evaluated exclusively on MIMIC-IV data from a single US academic medical center. Clinical practice, documentation standards, and terminology usage vary substantially across institutions and countries, and system performance on data from other centers—such as eICU, UK Biobank, or non-English-language EHR systems—remains unvalidated. Within the Discharge-Me benchmark itself, the current evaluation covers only `brief_hospital_course`; `discharge_instructions`, which requires reasoning over clinical guidelines and pharmacological knowledge rather than structured EHR fields, is not yet included in primary evaluation. Extending coverage to post-discharge instruction content and to other clinical document types (inpatient notes, radiology reports, surgical records) will require integration of external knowledge bases such as UMLS and SNOMED-CT, an approach supported by recent work on Medical Graph RAG [31] and healthcare RAG surveys [32].

### 9.2 Methodological Limitations

The knowledge graph is grounded exclusively in information explicitly recorded in EHRs and does not incorporate implicit medical knowledge such as drug interactions, contraindication rules, or disease progression patterns. This limits detection capability for complex statements requiring inferential verification: for example, a claim that “eGFR improvement led to medication discontinuation” represents clinical reasoning rather than a direct EHR fact, and the current system cannot reliably distinguish such causal claims from hallucinations. Synonym and abbreviation variation (e.g., “adult-onset diabetes” vs. “type 2 diabetes mellitus”) also causes missed E4 detections when standardization is incomplete. Temporal reasoning presents a further bottleneck: verifying statements such as “patient developed complications on post-op day 3” requires understanding temporal sequences and causal dependencies that exceed current graph query capabilities. Constructing knowledge graphs with timestamped edges and integrating causal reasoning mechanisms are important directions for future work.

### 9.3 Evaluation Limitations

The main experiment evaluates 50 held-out patients, which is sufficient to establish method-level performance benchmarks but may not capture the full variability of real clinical deployment. Larger-scale evaluation across hundreds to thousands of patients, ideally with multi-center data, is necessary to validate production stability. The generation-stage-as-ground-truth labeling strategy introduces a potential circularity concern, mitigated by the architectural independence of the generation and detection agents and by the grounding of labels in objective EHR facts; however, boundary cases may still be influenced by automated generation rules. Manual double-blind annotation by clinical experts on a representative subset remains as future validation work. Note that

the previously reported 97% agreement refers to automated labels versus manual review, rather than inter-annotator agreement among human experts. The current study also does not compare CuraView outputs against a physician-authored hallucination-detection workflow or measure physician time savings; those comparisons are necessary before claiming clinical workflow benefit. Finally, laboratory results have not been validated in actual clinical workflows, and the gap between controlled evaluation and real-world deployment—including interface integration, response latency requirements, and physician acceptance—remains to be characterized.

## 9.4 Computational and Ethical Considerations

Local deployment currently requires 8-bit quantization on NVIDIA RTX 4090-class hardware (24 GB VRAM); further compression via INT4 quantization or model distillation would broaden accessibility. GraphRAG indexing for the 250-patient subset requires approximately 30 minutes; scaling to tens of thousands of patients will require optimized graph storage and incremental indexing strategies. On the ethical side, knowledge graphs may indirectly expose patient information through entity associations even when source records are de-identified, necessitating differential privacy and federated learning mechanisms before real-world deployment. Full compliance verification with data protection regulations such as HIPAA and GDPR would be required prior to clinical deployment and is beyond the scope of the current research prototype. As an auxiliary decision-support tool, CuraView’s outputs must not replace physician judgment; clear accountability boundaries and regulatory frameworks for AI-assisted clinical documentation are required and currently institution-dependent. The 9.1% false-negative rate on E4 errors means that multi-layer safety mechanisms—mandatory manual review of low-confidence cases, continuous performance monitoring, and periodic re-evaluation—are essential complements to automated detection in any clinical deployment.

## References

- [1] Arun James Thirunavukarasu, Darren Shu Jeng Ting, Kabilan Elangovan, Laura Gutierrez, Ting Fang Tan, and Daniel Shu Wei Ting. Large language models in medicine. *Nature Medicine*, 29(8):1930–1940, 2023. doi: 10.1038/s41591-023-02448-8.
- [2] Peter Lee, Sebastien Bubeck, and Joseph Petro. Benefits, limits, and risks of GPT-4 as an AI chatbot for medicine. *New England Journal of Medicine*, 388(13):1233–1239, 2023. doi: 10.1056/NEJMs2214184.
- [3] Karan Singhal, Shekoofeh Azizi, Tao Tu, S Sara Mahdavi, Jason Wei, Hyung Won Chung, Nathan Scales, et al. Large language models encode clinical knowledge. *Nature*, 620(7972): 172–180, 2023. doi: 10.1038/s41586-023-06291-2.
- [4] Karan Singhal, Tao Tu, Juraj Gottweis, Rory Sayres, Ellery Wulczyn, Le Hou, Kevin Clark,

- et al. Towards expert-level medical question answering with large language models. *arXiv preprint arXiv:2305.09617*, 2023. URL <https://arxiv.org/abs/2305.09617>.
- [5] Harsha Nori, Nicholas King, Scott Mayer McKinney, Dean Carignan, and Eric Horvitz. Capabilities of GPT-4 on medical challenge problems. *arXiv preprint arXiv:2303.13375*, 2023. URL <https://arxiv.org/abs/2303.13375>.
- [6] Christopher Y. K. Williams, Charumathi Raghu Subramanian, Syed Salman Ali, et al. Physician- and large language model-generated hospital discharge summaries. *JAMA Internal Medicine*, 185(7):818–825, 2025. URL <https://jamanetwork.com/journals/jamainternalmedicine/fullarticle/2833228>.
- [7] Elham Asgari, Nina Montaña-Brown, Magda Dubois, Saleh Khalil, Jasmine Balloch, Joshua Au Yeung, and Dominic Pimenta. A framework to assess clinical safety and hallucination rates of LLMs for medical text summarisation. *NPJ Digital Medicine*, 8:274, 2025. doi: 10.1038/s41746-025-01670-7.
- [8] Hussam Alkaissi and Samy I McFarlane. Artificial hallucinations in ChatGPT: Implications in scientific writing. *Cureus*, 15(2):e35179, 2023. doi: 10.7759/cureus.35179.
- [9] Ziwei Ji, Nayeon Lee, Rita Frieske, Tiezheng Yu, Dan Su, Yan Xu, Etsuko Ishii, Ye Jin Bang, Andrea Madotto, and Pascale Fung. Survey of hallucination in natural language generation. *ACM Computing Surveys*, 55(12):1–38, 2023. doi: 10.1145/3571730.
- [10] Ankit Pal, Logesh Kumar Umapathi, and Malaikannan Sankarasubbu. Med-HALT: Medical domain hallucination test for large language models. In *Proceedings of the 27th Conference on Computational Natural Language Learning (CoNLL)*, pages 314–334, Singapore, 2023. Association for Computational Linguistics. URL <https://aclanthology.org/2023.conll-1.21/>.
- [11] Yaara Artsi, Eyal Klang, Jeremy D. Collins, Benjamin S. Glicksberg, Girish N. Nadkarni, Panagiotis Korfiatis, and Vera Sorin. Large language models in radiology reporting: A systematic review of performance, limitations, and clinical implications. *Intelligence-Based Medicine*, 12:100287, 2025. doi: 10.1016/j.ibmed.2025.100287.
- [12] Serena Zhang, Sraavya Sambara, Oishi Banerjee, Julian Acosta, L. John Fahrner, and Pranav Rajpurkar. RadFlag: A black-box hallucination detection method for medical vision language models. *arXiv preprint arXiv:2411.00299*, 2024. URL <https://arxiv.org/abs/2411.00299>.
- [13] Maya Rotmensch, Yoni Halpern, Abdulhakim Tlimat, Steven Horng, and David Sontag. Learning a health knowledge graph from electronic medical records. *Scientific Reports*, 7(1):5994, 2017. doi: 10.1038/s41598-017-05778-z.
- [14] Samuel G Finlayson, Paea LePendou, and Nigam H Shah. Building the graph of medicine from millions of clinical narratives. *Scientific Data*, 1:140032, 2014. doi: 10.1038/sdata.2014.32.

- [15] Darren Edge, Ha Trinh, Newman Cheng, Joshua Bradley, Alex Chao, Apurva Mody, Steven Truitt, and Jonathan Larson. From local to global: A graph RAG approach to query-focused summarization. *arXiv preprint arXiv:2404.16130*, 2024. URL <https://arxiv.org/abs/2404.16130>.
- [16] Patrick Lewis, Ethan Perez, Aleksandra Piktus, Fabio Petroni, Vladimir Karpukhin, Naman Goyal, Heinrich Küttler, et al. Retrieval-augmented generation for knowledge-intensive NLP tasks. In *Advances in Neural Information Processing Systems*, volume 33, pages 9459–9474, 2020. URL <https://arxiv.org/abs/2005.11401>.
- [17] Xiangru Tang, Anni Zou, Zhuosheng Zhang, Ziming Li, Yilun Zhao, Xingyao Zhang, Arman Cohan, and Mark Gerstein. MedAgents: Large language models as collaborators for zero-shot medical reasoning. *arXiv preprint arXiv:2311.10537*, 2023. URL <https://arxiv.org/abs/2311.10537>.
- [18] Harrison Chase. LangChain: Building applications with LLMs through composability, 2023. URL <https://github.com/langchain-ai/langchain>.
- [19] Yu Liu, Duantengchuan Li, Kaili Wang, Zhuoran Xiong, Fobo Shi, Jian Wang, Bing Li, and Bo Hang. Are LLMs good at structured outputs? A benchmark for evaluating structured output capabilities in LLMs. *Information Processing & Management*, 61(5):103809, 2024. doi: 10.1016/j.ipm.2024.103809.
- [20] Yaxi Lu, Haolun Li, Xin Cong, Zhong Zhang, Yesai Wu, Yankai Lin, Zhiyuan Liu, Fangming Liu, and Maosong Sun. Learning to generate structured output with schema reinforcement learning. In *Proceedings of the 63rd Annual Meeting of the Association for Computational Linguistics (Volume 1: Long Papers)*, pages 4905–4918, 2025. doi: 10.18653/v1/2025.acl-long.243.
- [21] Saibo Geng, Martin Josifoski, Maxime Peyrard, and Robert West. Grammar-constrained decoding for structured NLP tasks without finetuning. In *Proceedings of the 2023 Conference on Empirical Methods in Natural Language Processing*, pages 10932–10952, 2023. doi: 10.18653/v1/2023.emnlp-main.674.
- [22] Justin Xu, Zhihong Chen, Andrew Johnston, Louis Blankemeier, Maya Varma, Jason Hom, William J. Collins, Ankit Modi, Robert Lloyd, Benjamin Hopkins, Curtis Langlotz, and Jean-Benoit Delbrouck. Overview of the first shared task on clinical text generation: RRG24 and “Discharge Me!”. In *Proceedings of the 23rd Workshop on Biomedical Natural Language Processing*, pages 85–98, Bangkok, Thailand, 2024. Association for Computational Linguistics. doi: 10.18653/v1/2024.bionlp-1.7.
- [23] Stanford AIMI. Discharge Me! Stanford Center for Artificial Intelligence in Medicine and Imaging, 2024. URL <https://stanford-aimi.github.io/discharge-me/>.

- [24] Augustin Toma, Patrick R Lawler, Jimmy Ba, Rahul G Krishnan, Barry B Rubin, and Bo Wang. Clinical Camel: An open expert-level medical language model with dialogue-based knowledge encoding. *arXiv preprint arXiv:2305.12031*, 2023. URL <https://arxiv.org/abs/2305.12031>.
- [25] Chaoyi Wu, Xiaoman Zhang, Xin Zhang, Ya Wang, and Weidi Xie. PMC-LLaMA: Towards building open-source language models for medicine. *arXiv preprint arXiv:2304.14454*, 2023. URL <https://arxiv.org/abs/2304.14454>.
- [26] Haotian Wu, Paul Boulenger, Antonin Faure, Berta Céspedes, Farouk Boukil, Nastasia Morel, Zeming Chen, and Antoine Bosselut. EPFL-MAKE at “Discharge Me!”: An LLM system for automatically generating discharge summaries of clinical electronic health record. In *Proceedings of the 23rd Workshop on Biomedical Natural Language Processing*, pages 696–711, Bangkok, Thailand, 2024. Association for Computational Linguistics. doi: 10.18653/v1/2024.bionlp-1.61.
- [27] Mengxian Lyu, Cheng Peng, Daniel Paredes, Ziyi Chen, Aokun Chen, Jiang Bian, and Yonghui Wu. UF-HOBI at “Discharge Me!”: A hybrid solution for discharge summary generation through prompt-based tuning of GatorTronGPT models. *arXiv preprint arXiv:2407.15359*, 2024. URL <https://arxiv.org/abs/2407.15359>.
- [28] Luyu Gao, Zhuyun Dai, Panupong Pasupat, Anthony Chen, Arun Tejasvi Chaganty, Yicheng Fan, Vincent Y. Zhao, Ni Lao, Hongrae Lee, Da-Cheng Juan, and Kelvin Guu. RARR: Researching and revising what language models say, using language models. In *Proceedings of the 61st Annual Meeting of the Association for Computational Linguistics (Volume 1: Long Papers)*, pages 16477–16508, 2023. doi: 10.18653/v1/2023.acl-long.910.
- [29] Guangzhi Xiong, Qiao Jin, Zhiyong Lu, and Aidong Zhang. Benchmarking retrieval-augmented generation for medicine. *arXiv preprint arXiv:2402.13178*, 2024. URL <https://arxiv.org/abs/2402.13178>.
- [30] Chengrui Wang, Qingqing Long, Meng Xiao, Xunxin Cai, Chengjun Wu, Zhen Meng, Xuezhi Wang, and Yuanchun Zhou. BioRAG: A RAG-LLM framework for biological question reasoning. *arXiv preprint arXiv:2408.01107*, 2024. URL <https://arxiv.org/abs/2408.01107>.
- [31] Junde Wu, Jiayuan Zhu, Yunli Qi, Jingkun Chen, Min Xu, Filippo Menolascina, Yueming Jin, and Vicente Grau. Medical graph RAG: Evidence-based medical large language model via graph retrieval-augmented generation. In *Proceedings of the 63rd Annual Meeting of the Association for Computational Linguistics (Volume 1: Long Papers)*, pages 28443–28467, 2025. doi: 10.18653/v1/2025.acl-long.1381.
- [32] Lameck Mbangula Amugongo, Pietro Mascheroni, Steven Brooks, Stefan Doering, and Jan Seidel. Retrieval augmented generation for large language models in healthcare: A systematic review. *PLOS Digital Health*, 4(6):e0000877, 2025. doi: 10.1371/journal.pdig.0000877.

- [33] Olivier Bodenreider. The unified medical language system (UMLS): Integrating biomedical terminology. *Nucleic Acids Research*, 32(suppl\_1):D267–D270, 2004. doi: 10.1093/nar/gkh061.
- [34] Kevin Donnelly. SNOMED-CT: The advanced terminology and coding system for eHealth. *Studies in Health Technology and Informatics*, 121:279–290, 2006. URL <https://pubmed.ncbi.nlm.nih.gov/17095826/>.
- [35] World Health Organization. International statistical classification of diseases and related health problems 10th revision, 2016. URL <https://icd.who.int/browse10/2016/en>.
- [36] Eunsuk Chang and Sumi Sung. Use of SNOMED CT in large language models: Scoping review. *JMIR Medical Informatics*, 12:e62924, 2024. doi: 10.2196/62924.
- [37] Significant Gravitas. AutoGPT: An experimental open-source attempt to make GPT-4 fully autonomous, 2023. URL <https://github.com/Significant-Gravitas/AutoGPT>.
- [38] Shunyu Yao, Jeffrey Zhao, Dian Yu, Nan Du, Izhak Shafran, Karthik Narasimhan, and Yuan Cao. ReAct: Synergizing reasoning and acting in language models. *arXiv preprint arXiv:2210.03629*, 2023. URL <https://arxiv.org/abs/2210.03629>.
- [39] Weiwen Liu, Xu Huang, Xingshan Zeng, Xinlong Hao, Shuai Yu, Dexun Li, Shuai Wang, Weinan Gan, Zhengying Liu, Yuanqing Yu, et al. ToolACE: Winning the points of LLM function calling. *arXiv preprint arXiv:2409.00920*, 2025. URL <https://arxiv.org/abs/2409.00920>.
- [40] Akshara Prabhakar, Zuxin Liu, Weiran Yao, Jianguo Zhang, Ming Zhu, Shiyu Wang, Zhiwei Liu, Tulika Awalgaonkar, Haolin Chen, Thai Hoang, et al. APIGen-MT: Agentic pipeline for multi-turn data generation via simulated agent-human interplay. *arXiv preprint arXiv:2504.03601*, 2025. URL <https://arxiv.org/abs/2504.03601>.
- [41] Shaokun Zhang, Yi Dong, Jieyu Zhang, Jan Kautz, Bryan Catanzaro, Andrew Tao, Qingyun Wu, Zhiding Yu, and Guilin Liu. Nemotron-research-tool-N1: Exploring tool-using language models with reinforced reasoning. *arXiv preprint arXiv:2505.00024*, 2025. URL <https://arxiv.org/abs/2505.00024>.
- [42] Emily Croxford et al. Evaluating clinical AI summaries with large language models as judges. *NPJ Digital Medicine*, 8(1):640, 2025. doi: 10.1038/s41746-025-02005-2.
- [43] Selvan Sunitha Ravi, Bartosz Mielczarek, Anand Kannappan, Douwe Kiela, and Rebecca Qian. Lynx: An open source hallucination evaluation model. *arXiv preprint arXiv:2407.08488*, 2024. URL <https://arxiv.org/abs/2407.08488>.
- [44] Markus Frohmann, Igor Sterner, Ivan Vulić, Benjamin Minixhofer, and Markus Schedl. Segment any text: A universal approach for robust, efficient and adaptable sentence segmentation.

- In *Proceedings of the 2024 Conference on Empirical Methods in Natural Language Processing*, pages 11908–11941, Miami, Florida, USA, 2024. Association for Computational Linguistics. URL <https://aclanthology.org/2024.emnlp-main.665>.
- [45] LangChain. Structured output. LangChain Documentation, 2024. URL <https://docs.langchain.com/oss/python/langchain/structured-output>.
- [46] Zhouyu Jiang, Mengshu Sun, Zhiqiang Zhang, and Lei Liang. Bi’an: A bilingual benchmark and model for hallucination detection in retrieval-augmented generation. *arXiv preprint arXiv:2502.19209*, 2025. URL <https://arxiv.org/abs/2502.19209>.
- [47] Siya Qi, Rui Cao, Yulan He, and Zheng Yuan. Evaluating LLMs’ assessment of mixed-context hallucination through the lens of summarization. In *Findings of the Association for Computational Linguistics: ACL 2025*, pages 16480–16503, Vienna, Austria, 2025. Association for Computational Linguistics. doi: 10.18653/v1/2025.findings-acl.847.
- [48] Paulius Micikevicius, Sharan Narang, Jonah Alben, Gregory Diamos, Erich Elsen, David Garcia, Boris Ginsburg, Michael Houston, Oleksii Kuchaiev, Ganesh Venkatesh, and Hao Wu. Mixed precision training. *arXiv preprint arXiv:1710.03740*, 2018. URL <https://arxiv.org/abs/1710.03740>.
- [49] Kento Fujii, Satoshi Tamaki, Yusuke Kuroda, Ryota Shingaki, and Yutaka Kanemasa. Accelerating large language model training with 4D parallelism and memory consumption estimator. *arXiv preprint arXiv:2411.06465*, 2024. URL <https://arxiv.org/abs/2411.06465>.
- [50] Junyeob Kim, Junho Kim, Hwanju Kim, and Jangwoo Kim. LLMem: Estimating GPU memory usage for fine-tuning pre-trained LLMs. *arXiv preprint arXiv:2404.10933*, 2024. URL <https://arxiv.org/abs/2404.10933>.
- [51] An Yang, Anfeng Li, Baosong Yang, Beichen Zhang, Binyuan Hui, et al. Qwen3 technical report. *arXiv preprint arXiv:2505.09388*, 2025. URL <https://arxiv.org/abs/2505.09388>.
- [52] Zeming Chen, Alejandro Hernández-Cano, Angelika Romanou, Antoine Bonnet, Kyle Matoba, Francesco Salvi, Matteo Pagliardini, et al. MEDITRON-70B: Scaling medical pretraining for large language models. *arXiv preprint arXiv:2311.16079*, 2023. URL <https://arxiv.org/abs/2311.16079>.